Phenomenology of $b \to c\tau\bar{\nu}$ decays in a scalar leptoquark model*

Han Yan(颜涵)[1] Ya-Dong Yang(杨亚东)[2] Xing-Bo Yuan(袁兴博)[3]

Institute of Particle Physics and Key Laboratory of Quark and Lepton Physics (MOE), Central China Normal University, Hubei 430079, China

Abstract: During the past few years, signs of lepton flavor universality (LFU) violation have been observed in $b \to c\tau\bar{\nu}$ and $b \to s\ell^+\ell^-$ transitions. Recently, the D^* and τ polarization fractions $P_L^{D^*}$ and P_L^τ in $B \to D^*\tau\bar{\nu}$ decay were likewise measured by the Belle collaboration. Motivated by these intriguing results, we revisit the $R_{D^{(*)}}$ and $R_{K^{(*)}}$ anomalies in a scalar leptoquark (LQ) model, where two scalar LQs, one of which is a $SU(2)_L$ singlet and the other a $SU(2)_L$ triplet, are introduced simultaneously. We consider five $b \to c\tau\bar{\nu}$ mediated decays, $B \to D^{(*)}\tau\bar{\nu}$, $B_c \to \eta_c\tau\bar{\nu}$, $B_c \to J/\psi\tau\bar{\nu}$, and $\Lambda_b \to \Lambda_c\tau\bar{\nu}$, and focus on the LQ effects on the q^2 distributions of the branching fractions, LFU ratios, and various angular observables in these decays. Under the combined constraints of the available data on $R_{D^{(*)}}$, $R_{J/\psi}$, $P_L^\tau(D^*)$, and $P_L^{D^*}$, we perform scans for the LQ couplings and make predictions for a number of observables. Numerically it is found that both the differential branching fractions and LFU ratios are largely enhanced by the LQ effects, with the latter expected to provide testable signatures at the SuperKEKB and High-Luminosity LHC experiments.

Keywords: new physics, leptoquark, B decay

PACS: 13.25.Hw, 13.30.Ce **DOI:** 10.1088/1674-1137/43/8/083105

1 Introduction

To date, the LHC has not provided any direct evidence for new physics (NP) particles beyond the standard model (SM). However, several hints referring to the lepton flavor university (LFU) violation emerge in the measurements of semileptonic b-hadron decays, which, if confirmed with more precise experimental data and theoretical predictions, depict unambiguous signs of NP [1, 2].

The charged-current decays $B \to D^{(*)}l\bar{\nu}$, with $\ell = e$, μ, or τ, have been measured by the BaBar [3, 4], Belle [5–8], and LHCb [9–11] collaborations. The ratios of the branching fractions[4], $R_{D^{(*)}} \equiv \mathcal{B}(B \to D^{(*)}\tau\bar{\nu})/\mathcal{B}(B \to D^{(*)}\ell\bar{\nu})$, with $\ell = e$ and/or μ, obtained by the latest experimental averages by the heavy flavor averaging group read [12]

$$R_D^{\rm exp} = 0.407 \pm 0.039\,({\rm stat.}) \pm 0.024\,({\rm syst.}), \quad (1)$$

$$R_{D^*}^{\rm exp} = 0.306 \pm 0.013\,({\rm stat.}) \pm 0.007\,({\rm syst.}), \quad (2)$$

both of which exceed their respective SM predictions [12][5]

$$R_D^{\rm SM} = 0.299 \pm 0.003, \quad R_{D^*}^{\rm SM} = 0.258 \pm 0.005, \quad (3)$$

by 2.3σ and 3.0σ, respectively. Considering the experimental correlation of -0.203 between R_D and R_{D^*}, the combined results exhibit a $\sim 3.78\sigma$ deviation from the SM predictions [12]. This discrepancy, referred to as the $R_{D^{(*)}}$ anomaly, may provide a hint of LFU violating NP [1, 2]. For the $B_c \to J/\psi\ell\bar{\nu}$ decay, a ratio $R_{J/\psi}$ can be similarly defined. The recent LHCb measurement, $R_{J/\psi}^{\rm exp} = 0.71 \pm 0.17\,({\rm stat.}) \pm 0.18\,({\rm syst.})$ [17], lies about 2σ above the SM prediction, $R_{J/\psi}^{\rm SM} = 0.248 \pm 0.006$ [18]. In addition, the LHCb measurements of the ratios $R_{K^{(*)}} \equiv \mathcal{B}(B \to K^{(*)}\mu^+\mu^-)/\mathcal{B}(B \to K^{(*)}e^+e^-)$, $R_K^{\rm exp} = 0.745^{+0.090}_{-0.074} \pm 0.036$ for $1.0\,{\rm GeV}^2 \leqslant q^2 \leqslant 6.0\,{\rm GeV}^2$ [19] and $R_{K^*}^{\rm exp} = 0.69^{+0.11}_{-0.07} \pm 0.05$ for $1.1\,{\rm GeV}^2 \leqslant q^2 \leqslant 6.0\,{\rm GeV}^2$ [20], are found to be about 2.6σ and $\sim 2.5\sigma$ lower than the SM expectation, $R_{K^{(*)}}^{\rm SM} \simeq 1$ [21, 22], respect-

Received 21 March 2019, Published online 26 June 2019

* Supported by the National Natural Science Foundation of China (11775092, 11521064, 11435003, 11805077). XY is also supported in part by the startup research funding from CCNU

1) E-mail: yanhan@mails.ccnu.edu.cn

2) E-mail: yangyd@mail.ccnu.edu.cn

3) E-mail: y@mail.ccnu.edu.cn

4) Compared to the branching fractions themselves, the ratios $R_{D^{(*)}}$ are advantaged by the fact that, apart from significant reduction of the experimental systematic uncertainties, the CKM matrix element V_{cb} cancels out and the sensitivity to $B \to D^{(*)}$ transition form factors becomes much weaker.

5) Here the SM values are the arithmetic averages [12] of the most recent calculations by several groups [13–16].

ively. These anomalies motivated numerous studies both in the effective field theory approach [23–28] and in specific NP models [29–45]. We refer to Refs. [1, 2] for recent reviews.

Recently, the Belle collaboration reported the first preliminary result of the D^* longitudinal polarization fraction in the $B \to D^* \tau \bar{\nu}$ decay [46, 47]

$$P_L^{D^*} = 0.60 \pm 0.08\,(\text{stat.}) \pm 0.04\,(\text{syst.}), \tag{4}$$

which is consistent with the SM prediction $P_L^{D^*} = 0.46 \pm 0.04$ [48] at 1.5σ. Together with the measurements of the τ polarization, $P_L^{\tau} = -0.38 \pm 0.51\,(\text{stat.})^{+0.21}_{-0.16}\,(\text{syst.})$ [7, 8], these results provide valuable information on the spin structure of the interaction involved in $B \to D^{(*)} \tau \bar{\nu}$ decays and are good observables for testing of various NP scenarios [48– 53]. The measurement of angular observables in these decays will be considerably improved in the future [54, 55]. For example, the Belle II experiment with $50\,\text{ab}^{-1}$ data can measure P_L^{τ} with an expected precision of ± 0.07 [54].

In this work, motivated by these experimental progresses and future prospects, we study five $b \to c\tau\bar{\nu}$ decays, $B \to D^{(*)}\tau\bar{\nu}$, $B_c \to \eta_c \tau\bar{\nu}$, $B_c \to J/\psi\tau\bar{\nu}$, and $\Lambda_b \to \Lambda_c \tau\bar{\nu}$, in the leptoquark (LQ) model proposed in Ref. [56]. Models with one or more LQ states, which are colored bosons that couple to both quarks and leptons, depict some of the most popular scenarios employed to explain the $R_{D^{(*)}}$ and $R_{K^{(*)}}$ anomalies [57–74]. In Ref. [56], the SM is extended with two scalar LQs, one of which is a $SU(2)_L$ singlet, whereas the other is a $SU(2)_L$ triplet. This model is also featured by the fact that these two LQs have the same mass and hypercharge, and their couplings to fermions are related by a discrete symmetry. In this manner, the anomalies in $b \to c\tau\bar{\nu}$ and $b \to s\mu^+\mu^-$ transitions can be explained simultaneously, while avoiding potentially dangerous contributions to $b \to s\nu\bar{\nu}$ decays. By taking into account recent developments on transition form factors [13, 14, 18, 75–77], we derive constraints on LQ couplings in this model. Subsequently, predictions in the LQ model are made for the five $b \to c\tau\bar{\nu}$ decays, focusing on the q^2 distributions of the branching fractions, LFU ratios, and various angular observables. Implications for future research at the High-Luminosity LHC (HL-LHC) [78] and SuperKEKB [54] are also briefly discussed.

This paper is organized as follows: in Section 2, we provide a brief review of the LQ model proposed in Ref. [56]. In Section 3, we recapitulate the theoretical formulae for the various flavor processes and discuss the LQ effects on these decays. In Section 4, we present our detailed numerical analysis and discussions. Our conclusions are given in Section 5. The relevant transition form factors and helicity amplitudes are presented in the appendices.

2 Model

In this section, we recapitulate the LQ model proposed in Ref. [56], where a scalar LQ singlet Φ_1 and a triplet Φ_3 are added to the SM field content, to explain the observed flavor anomalies. Under the SM gauge group $(SU(3)_C, SU(2)_L, U(1)_Y)$, the LQ states Φ_1 and Φ_3 transform as $(\mathbf{3}, \mathbf{1}, -\mathbf{2/3})$ and $(\mathbf{3}, \bar{\mathbf{3}}, -\mathbf{2/3})$, respectively. Their interactions with the SM fermions are described by the Lagrangian [56]

$$\mathcal{L} = \lambda^{1L}_{jk} \bar{Q}^c_j i\tau_2 L_k \Phi_1^\dagger + \lambda^{3L}_{jk} \bar{Q}^c_j i\tau_2 (\tau \cdot \Phi_3)^\dagger L_k + \text{h.c.}, \tag{5}$$

where Q_j and L_k denote the left-handed quark and lepton doublet with generation indices j and k, respectively. The couplings λ^{1L}_{jk} and λ^{3L}_{jk} are generally complex, however assumed to be real throughout this work. It is further assumed that these two scalar LQs have the same mass M, and their couplings to the SM fermions satisfy the following discrete symmetry [56]:

$$\lambda^L_{jk} \equiv \lambda^{1L}_{jk}, \qquad \lambda^{3L}_{jk} = e^{i\pi j} \lambda^L_{jk}. \tag{6}$$

With these two assumptions, the tree-level LQ contributions to the $b \to s\nu\bar{\nu}$ decays are canceled. After rotating to the mass eigenstate basis, the LQ couplings to the left-handed quarks involve the CKM elements as

$$\lambda^L_{d_j k} = \lambda^L_{jk}, \qquad \lambda^L_{u_j k} = V^*_{ji} \lambda^L_{ik}, \tag{7}$$

where V_{ij} is the CKM matrix element.

3 Theoretical framework

In this section, we introduce the theoretical framework for the relevant flavor processes and discuss the LQ effects on these decays.

3.1 $b \to c\tau\bar{\nu}$ mediated processes

Including the LQ contributions, the effective Hamiltonian responsible for $b \to c\ell_i \bar{\nu}_j$ transitions is given by [56]

$$\mathcal{H}_{\text{eff}} = \frac{4G_F}{\sqrt{2}} V_{cb} C_L^{ij} (\bar{c}\gamma^\mu P_L b)(\bar{\ell}_i \gamma_\mu P_L \nu_j), \tag{8}$$

with the Wilson coefficient $C_L^{ij} = C_L^{\text{SM},ij} + C_L^{\text{NP},ij}$. The W-exchange contribution within the SM yields $C_L^{\text{SM},ij} = \delta_{ij}$, and the LQ contributions result in

$$C_L^{\text{NP},ij} = \frac{\sqrt{2}}{8 G_F M^2} \frac{V_{ck}}{V_{cb}} \lambda^L_{3j} \lambda^{L*}_{ki} \left[1 + (-1)^k\right]. \tag{9}$$

This Wilson coefficient is given at the matching scale $\mu_{\text{NP}} \sim M$. However, as the corresponding current is conserved, we can obtain the low-energy Wilson coefficient, $C_L^{\text{NP},ij}(\mu_b) = C_L^{\text{NP},ij}$, without considering the renormalization group evolution (RGE) effect.

In this study, we consider five processes mediated by

the quark-level $b\to c\ell\bar{\nu}$ transition, including $B\to D^{(*)}\ell\bar{\nu}$, $B_c\to\eta_c\ell\bar{\nu}$, $B_c\to J/\psi\ell\bar{\nu}$, and $\Lambda_b\to\Lambda_c\ell\bar{\nu}$ decays. All these processes can be uniformly represented by

$$M(p_M,\lambda_M)\to N(p_N,\lambda_N)+\ell^-(p_\ell,\lambda_\ell)+\bar{\nu}_\ell(p_{\bar{\nu}_\ell}), \tag{10}$$

where $(M,N)=(B,D^{(*)}),(B_c,\eta_c),(B_c,J/\psi)$, and (Λ_b,Λ_c), and $(\ell,\bar{\nu})=(e,\bar{\nu}_e),(\mu,\bar{\nu}_\mu)$, and $(\tau,\bar{\nu}_\tau)$. For each particle i in the above decay, its momentum and helicity are denoted by p_i and λ_i, respectively. In particular, the helicity of a pseudoscalar meson is zero, i.e., $\lambda_{B_{(c)},D,\eta_c}=0$. After averaging over the non-zero helicity of the hadron M, the differential decay rate of this process can be written as [53, 79]

$$\mathrm{d}\Gamma^{\lambda_N,\lambda_\ell}(M\to N\ell^-\bar{\nu}_\ell)=\frac{1}{2m_M}\frac{1}{2|\lambda_M|+1}\sum_{\lambda_M}|\mathcal{M}^{\lambda_M}_{\lambda_N,\lambda_\ell}|^2\mathrm{d}\Phi_3, \tag{11}$$

with the phase space

$$\mathrm{d}\Phi_3=\frac{\sqrt{Q_+Q_-}}{256\pi^3m_M^2}\sqrt{1-\frac{m_\ell^2}{q^2}}\mathrm{d}q^2\mathrm{d}\cos\theta_\ell, \tag{12}$$

where $Q_\pm=m_\pm^2-q^2$, with $m_\pm=m_M\pm m_N$ and q^2 depicts the dilepton invariant mass squared. $\theta_\ell\in[0,\pi]$ denotes the angle between the three-momentum of ℓ and that of N in the ℓ-$\bar{\nu}$ center-of-mass frame. The helicity amplitudes $\mathcal{M}^{\lambda_M}_{\lambda_N,\lambda_\ell}\equiv\langle N\ell\bar{\nu}_\ell|\mathcal{H}_{\rm eff}|M\rangle$ can be written as [76]

$$\begin{aligned}\mathcal{M}^{\lambda_M}_{\lambda_N,\lambda_\tau}=&\frac{G_FV_{cb}}{\sqrt{2}}\Big(H^{SP}_{\lambda_M,\lambda_N}L^{SP}_{\lambda_\tau}+\sum_{\lambda_W}\eta_{\lambda_W}H^{VA}_{\lambda_M,\lambda_N,\lambda_W}L^{VA}_{\lambda_\tau,\lambda_W}\\&+\sum_{\lambda_{W_1},\lambda_{W_2}}\eta_{\lambda_{W_1}}\eta_{\lambda_{W_2}}H^{T}_{\lambda_M,\lambda_N,\lambda_{W_1},\lambda_{W_2}}L^{T}_{\lambda_\tau,\lambda_{W_1}\lambda_{W_2}}\Big),\end{aligned} \tag{13}$$

where λ_{W_i} denotes the helicity of the virtual vector bosons W, W_1 and W_2. The coefficient $\eta_{\lambda_{W_i}}=1$ for $\lambda_{\lambda_{W_i}}=t$, and $\eta_{\lambda_{W_i}}=-1$ for $\lambda_{\lambda_{W_i}}=0,\pm1$. Explicit analytical expressions of the leptonic and hadronic helicity amplitudes H and L are given in appendices A and C.

From Eq. (11), we can derive the following observables:

• The differential decay width and branching fraction

$$\begin{aligned}\frac{\mathrm{d}\mathcal{B}(M\to N\ell\bar{\nu}_\ell)}{\mathrm{d}q^2}=&\frac{1}{\Gamma_M}\frac{\mathrm{d}\Gamma(M\to N\ell\bar{\nu}_\ell)}{\mathrm{d}q^2}\\=&\frac{1}{\Gamma_M}\sum_{\lambda_N,\lambda_\ell}\frac{\mathrm{d}\Gamma^{\lambda_N,\lambda_\ell}(M\to N\ell\bar{\nu}_\ell)}{\mathrm{d}q^2},\end{aligned} \tag{14}$$

where $\Gamma_M=1/\tau_M$ is the total width of the hadron M.

• The q^2-dependent LFU ratio

$$R_N(q^2)=\frac{\mathrm{d}\Gamma(M\to N\tau\bar{\nu}_\tau)/\mathrm{d}q^2}{\mathrm{d}\Gamma(M\to Nl\bar{\nu}_l)/\mathrm{d}q^2}, \tag{15}$$

where $\mathrm{d}\Gamma(M\to Nl\bar{\nu}_l)/\mathrm{d}q^2$ denotes the average of the different decay widths of the electronic and muonic modes.

• The lepton forward-backward asymmetry

$$A_{\rm FB}(q^2)=\frac{\int_0^1\mathrm{d}\cos\theta_\ell(\mathrm{d}^2\Gamma/\mathrm{d}q^2\mathrm{d}\cos\theta_\ell)-\int_{-1}^0\mathrm{d}\cos\theta_\ell(\mathrm{d}^2\Gamma/\mathrm{d}q^2\mathrm{d}\cos\theta_\ell)}{\mathrm{d}\Gamma/\mathrm{d}q^2}. \tag{16}$$

• The q^2-dependent polarization fractions

$$\begin{aligned}P_L^\tau(q^2)=&\frac{\mathrm{d}\Gamma^{\lambda_\tau=+1/2}/\mathrm{d}q^2-\mathrm{d}\Gamma^{\lambda_\tau=-1/2}/\mathrm{d}q^2}{\mathrm{d}\Gamma/\mathrm{d}q^2},\\P_L^N(q^2)=&\frac{\mathrm{d}\Gamma^{\lambda_N=+1/2}/\mathrm{d}q^2-\mathrm{d}\Gamma^{\lambda_N=-1/2}/\mathrm{d}q^2}{\mathrm{d}\Gamma/\mathrm{d}q^2},\ \text{for } N=\Lambda_c,\\P_L^N(q^2)=&\frac{\mathrm{d}\Gamma^{\lambda_N=0}/\mathrm{d}q^2}{\mathrm{d}\Gamma/\mathrm{d}q^2},\ \text{for } N=D^*,J/\psi,\\P_T^N(q^2)=&\frac{\mathrm{d}\Gamma^{\lambda_N=1}/\mathrm{d}q^2-\mathrm{d}\Gamma^{\lambda_N=-1}/\mathrm{d}q^2}{\mathrm{d}\Gamma/\mathrm{d}q^2},\ \text{for } N=D^*,J/\psi.\end{aligned} \tag{17}$$

Analytical expressions of all the above observables are given in Appendix C. As these angular observables depict ratios of the decay widths, they are largely free of hadronic uncertainties and thus provide excellent tests of the NP effects.

As shown in Eq. (8), LQ effects generate an operator with the same chirality structure as in the SM. Therefore, it is straightforward to derive the following relation:

$$\frac{R_N}{R_N^{\rm SM}}=\sum_{i=1}^3\left|\delta_{3i}+C_L^{3i}\right|^2, \tag{18}$$

with $N=D^{(*)},\eta_c,J/\psi$ and Λ_c. Here, vanishing contributions to the electronic and muonic channels are already assumed.

One of the main inputs in our calculations are the transition form factors. In this respect, notable progresses have been achieved in recent years [13–16, 75–77, 80–87]. This study adopts the Boyd-Grinstein-Lebed (BGL) [13, 88] and Caprini-Lellouch-Neubert (CLN) [14, 89] parametrization for the $B\to D$ and $B\to D^*$ transition form factors, respectively. In these approaches, both the transition form factors and the CKM matrix element $|V_{cb}|$ are simultaneously extracted from the experimental data. In addition, we use the $B_c\to\eta_c,J/\psi$ transition form factors obtained in the covariant light-front approach [18]. For the $\Lambda_b\to\Lambda_c$ transition form factor, we adopt the recent Lattice QCD results in Refs. [75, 76]. Explicit expressions of all the relevant transition form factors are recapitulated in Appendix B.

3.2 Other processes

With the LQ effects considered, the effective Hamiltonian for the $b\to s\ell_i^+\ell_j^-$ transition can be written as [90]

$$\mathcal{H}_{\rm eff}=-\frac{4G_F}{\sqrt{2}}V_{tb}V_{ts}^*\sum_aC_a^{ij}O_a^{ij}+\text{h.c.}, \tag{19}$$

where the operators relevant to our study are

$$O_9^{ij} = \frac{\alpha_e}{4\pi}(\bar{s}\gamma^\mu P_L b)(\bar{\ell}_i\gamma_\mu \ell_j),$$
$$O_{10}^{ij} = \frac{\alpha_e}{4\pi}(\bar{s}\gamma^\mu P_L b)(\bar{\ell}_i\gamma_\mu\gamma^5 \ell_j). \quad (20)$$

The LQ contributions result in [56]

$$C_9^{\mathrm{NP},ij} = -C_{10}^{\mathrm{NP},ij} = \frac{-\sqrt{2}}{2G_F V_{tb}V_{ts}^*}\frac{\pi}{\alpha_e}\frac{1}{M^2}\lambda_{3j}^L\lambda_{2i}^{L*}. \quad (21)$$

In the model-independent approach, the current $b\to s\mu^+\mu^-$ anomalies can be explained by a $C_9^{\mathrm{NP},22} = -C_{10}^{\mathrm{NP},22}$ -like contribution, with the permitted range given by [91–93]

$$-0.91\,(-0.71) \leqslant C_9^{\mathrm{NP},22} = -C_{10}^{\mathrm{NP},22} \leqslant -0.18\,(-0.35), \quad (22)$$

at the 2σ (1σ) level, which in turn sets a constraint on $\lambda_{22}^{L*}\lambda_{32}^L$. Furthermore, the LQ contributions to $b\to s\tau^+\tau^-$ and $b\to c\tau\bar{\nu}_\tau$ transitions depend on the same product $\lambda_{23}^{L*}\lambda_{33}^L$, therefore making a direct correlation between the branching fraction $\mathcal{B}(B_s\to\tau^+\tau^-)$ and $R_{D^{(*)}}$.

For the $b\to s\nu\bar{\nu}$ transitions, both the LQs Φ_1 and Φ_3 generate tree-level contributions. However, assuming that they have the same mass, their effects are canceled out due to the discrete symmetry in Eq. (6). In addition, this LQ scenario can accommodate the $(g-2)_\mu$ anomaly [94, 95], once the right-handed interaction term $\lambda_{fi}^R\bar{u}_f^c\ell_i\Phi_1^\dagger$ is introduced to Eq. (5) [56]. We do not consider such a term in this study. Further details can be found in Ref. [56], where various lepton flavor violating decays of leptons and B meson have also been discussed.

Finally, we provide brief comments on direct searches for the LQs at high-energy colliders. Because the LQ contributions to $b\to c\tau\bar{\nu}$ transitions only involve the product $\lambda_{23}^{L*}\lambda_{33}^L$, searches for the LQs with couplings to the second and third generations are more relevant to our work. At the LHC, both the CMS and ATLAS collaborations have performed searches for such LQs in several channels, e.g., LQ $\to t\mu$ [96], LQ $\to t\tau$ [97], LQ $\to b\tau$ [97], etc. Current results from the LHC have excluded the LQs with masses below about 1 TeV [95]. For example, searches for pair-produced scalar LQs decaying into t quark and μ lepton have been performed by the CMS Collaboration, in which a scalar LQ with mass below 1420 GeV was excluded at 95% CL under the assumption of $\mathcal{B}(\mathrm{LQ}\to t\mu)=1$ [96]. All these collider constraints depend on the assumption of the total width of the LQ, which involves all the LQ couplings λ_{ij}^L. To apply the collider constraints to our scenario, one needs to perform a global fit on all the LQ couplings and derive bounds on the total width. Such analysis is beyond the scope of this study. Regarding the scenario with one singlet and one triplet LQ, we refer to Ref. [72] for a more detailed collider analysis. Furthermore, our analysis does not depend on the mass of the LQ, because LQ couplings always appear in the form of $\lambda_{23}^{L*}\lambda_{33}^L/M^2$ in $b\to c\tau\bar{\nu}$ transitions, as in Eq. (9).

4 Numerical analysis

In this section, we present our numerical analysis of the LQ effects on the decays considered. After deriving the constraints of the model parameters, we concentrate on the LQ effects on the five $b\to c\tau\bar{\nu}$ decays, i.e., $B\to D^{(*)}\tau\bar{\nu}$, $B_c\to\eta_c\tau\bar{\nu}$, $B_c\to J/\psi\tau\bar{\nu}$, and $\Lambda_b\to\Lambda_c\tau\bar{\nu}$.

4.1 SM predictions

In Table 1, we list the relevant input parameters used in our numerical analysis. Using the theoretical framework described in Section 3, the SM predictions for $B\to D^{(*)}\tau\bar{\nu}$, $B_c\to\eta_c\tau\bar{\nu}$, $B_c\to J/\psi\tau\bar{\nu}$, and $\Lambda_b\to\Lambda_c\tau\bar{\nu}$ decays are given in Table 2. To obtain the theoretical uncertainties, we vary each input parameter within their respective 1σ range and add each individual uncertainty in quadrature. Correlations among fit parameters were considered to obtain uncertainties of the transition form factors. In particular, for the $\Lambda_b\to\Lambda_c\tau\bar{\nu}$ decay, we follow the treatment of Ref. [75] to obtain the statistical and systematic uncertainties induced by the $\Lambda_b\to\Lambda_c$ transition form factors. From Table 2, the experimental data on the ratios R_D, R_{D^*}, and $R_{J/\psi}$ are found to deviate from the SM predictions by 2.31σ, 2.85σ and 1.83σ, respectively.

Table 1. Input parameters used in our numerical analysis.

input	value	unit	Ref.
$\alpha_s(m_Z)$	0.1181 ± 0.0011		[95]
m_t^{pole}	173.1 ± 0.9	GeV	[95]
$m_b(m_b)$	4.18 ± 0.03	GeV	[95]
$m_c(m_c)$	1.275 ± 0.025	GeV	[95]
$\lvert V_{cb}\rvert$(semi-leptonic)	$41.00\pm0.33\pm0.74$	10^{-3}	[98]
$\lvert V_{ub}\rvert$(semi-leptonic)	$3.98\pm0.08\pm0.22$	10^{-3}	[98]

4.2 Constraints

To obtain the permitted ranges of LQ parameters, we impose the experimental constraints in the same manner as in Refs. [99, 100]; i.e., for each point in the parameter space, if the difference between the corresponding theoretical prediction and experimental data is less than 2σ (3σ) error bar, which is calculated by adding the theoretical and experimental uncertainties in quadrature, this point is regarded as permitted at 2σ (3σ) level.

In the LQ scenario introduced in Section 2, the LQ contributions to $b\to c\tau\bar{\nu}$ transitions are all controlled by

Table 2. Predictions for branching fractions (in units of 10^{-2}) and ratios R_N of the five $b \to c\tau\bar{\nu}$ decay modes in the SM and the LQ scenario. The entry "—" indicates that no measurement is yet available for the corresponding observable.

observable	SM	NP	exp	Ref
$\mathcal{B}(B \to D\tau\bar{\nu})$	$0.711^{+0.042}_{-0.041}$	[0.702, 0.991]	0.90 ± 0.24	[95]
R_D	$0.301^{+0.003}_{-0.003}$	[0.313, 0.400]	$0.407 \pm 0.039 \pm 0.024$	[12]
$\mathcal{B}(B_c \to \eta_c\tau\bar{\nu})$	$0.204^{+0.024}_{-0.024}$	[0.188, 0.299]	–	
R_{η_c}	$0.281^{+0.035}_{-0.031}$	[0.263, 0.416]	–	
$\mathcal{B}(B \to D^*\tau\bar{\nu})$	$1.261^{+0.087}_{-0.085}$	[1.234, 1.788]	1.78 ± 0.16	[95]
R_{D^*}	0.258 ± 0.008	[0.263, 0.351]	$0.306 \pm 0.013 \pm 0.007$	[12]
P_L^τ	-0.503 ± 0.013	[−0.516, −0.490]	$-0.38 \pm 0.51^{+0.21}_{-0.16}$	[7, 8]
$P_L^{D^*}$	0.453 ± 0.012	[0.441, 0.465]	$0.60 \pm 0.08 \pm 0.04$	[46, 47]
$\mathcal{B}(B_c \to J/\psi\tau\bar{\nu})$	$0.398^{+0.045}_{-0.049}$	[0.366, 0.583]	–	
$R_{J/\psi}$	$0.248^{+0.006}_{-0.005}$	[0.255, 0.335]	$0.71 \pm 0.17 \pm 0.18$	[17]
$\mathcal{B}(\Lambda_b \to \Lambda_c\tau\bar{\nu})$	$1.762^{+0.105}_{-0.104}$	[1.737, 2.457]	–	
R_{Λ_c}	$0.333^{+0.010}_{-0.010}$	[0.339, 0.451]	–	

the product $\lambda_{23}^{L*}\lambda_{33}^{L}$. In the following analysis, the couplings λ_{23}^{L} and λ_{33}^{L} are assumed to be real. After considering the current experimental measurements of $R_{D^{(*)}}$, $R_{J/\psi}$, $P_L^\tau(D^*)$, and $P_L^{D^*}$, we find that the constraints on $\lambda_{23}^{L*}\lambda_{33}^{L}$ are dominated by R_D and R_{D^*}. The permitted ranges of $\lambda_{23}^{L*}\lambda_{33}^{L}$ at 2σ level are obtained as follows

$$-2.90 < \lambda_{23}^{L*}\lambda_{33}^{L} < -2.74, \quad \text{or} \quad 0.03 < \lambda_{23}^{L*}\lambda_{33}^{L} < 0.20, \quad (23)$$

where a common LQ mass $M = 1\,\text{TeV}$ is assumed. The solution with negative $\lambda_{23}^{L*}\lambda_{33}^{L}$ corresponds to the case in which the LQ interactions dominate over the SM contributions. We do not pursue this possibility in the following analysis. For the solution with positive $\lambda_{23}^{L*}\lambda_{33}^{L}$, the permitted regions of $(\lambda_{23}^{L}, \lambda_{33}^{L})$ at both 2σ and 3σ levels are shown in Fig. 1. In this figure, we also show the individual constraint from the D^* polarization fraction $P_L^{D^*}$, which remains weaker than the ones from $R_{D^{(*)}}$. In addition, the current measurement of the τ polarization fraction P_L^τ in $B \to D^*\tau\nu$ decay cannot provide any relevant constraint.

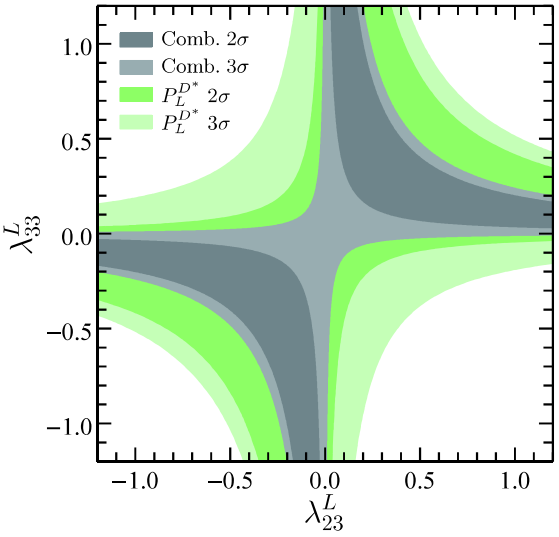

Fig. 1. (color online) Combined constraints on $(\lambda_{23}^{L}, \lambda_{33}^{L})$ by all $b \to c\tau\bar{\nu}$ processes at 2σ (black) and 3σ (gray) levels. The dark (light) green area indicates the allowed region by $P_L^{D^*}$ only at 2σ (3σ).

As mentioned in Section 3, the LQ contributions to $b \to s\tau^+\tau^-$ and $b \to c\tau\bar{\nu}_\tau$ depend on the same product

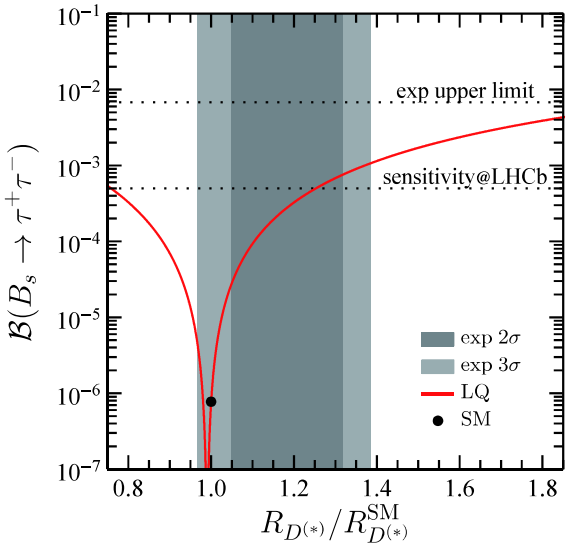

Fig. 2. (color online) Correlation between $R_{D^{(*)}}/R_{D^{(*)}}^{\rm SM}$ and $\mathcal{B}(B_s \to \tau^+\tau^-)$. The black (gray) region denotes the 2σ (3σ) experimental ranges of $R_{D^{(*)}}/R_{D^{(*)}}^{\rm SM}$. The horizontal dashed and dotted lines correspond to the current LHCb upper limit and the expected sensitivity by the end of LHCb Upgrade II, respectively. The black point indicates the SM prediction.

$\lambda_{23}^{L*}\lambda_{33}^{L}$. In the case of positive $\lambda_{23}^{L*}\lambda_{33}^{L}$, we show in Fig. 2 the correlation between $R_{D^{(*)}}/R_{D^{(*)}}^{\rm SM}$ and $\mathcal{B}(B_s\to\tau^+\tau^-)$. The LQ effects enhance the branching fraction of $B_s\to\tau^+\tau^-$ in most of the parameter space. At present, the experimental upper limit 6.8×10^{-3} [101] is far above the SM prediction $(7.73\pm0.49)\times10^{-7}$ [102]. However, to obtain the 2σ experimental range of $R_{D^{(*)}}$, the LQ contributions enhance $\mathcal{B}(B_s\to\tau^+\tau^-)$ by about 2–3 orders of magnitude compared to the SM prediction, which reaches the expected LHCb sensitivity 5×10^{-4} by the end of Upgrade II [55, 103]. The $B\to K^{(*)}\tau^+\tau^-$ decay may also play an important role in probing the LQ effects. Although the Belle II experiment would improve the current upper limit 2.25×10^{-3} at a 90% confidence level by no more than two orders of magnitude, the proposed FCC-*ee* collider can yield a few thousand of $B^0\to K^{*0}\tau^+\tau^-$ events from $O(10^{13})$ Z decays [104].

4.3 Predictions

Using the constrained parameter space at the 2σ level derived in the last subsection, we present predictions for the five $b\to c\tau\bar{\nu}$ processes. Table 2 shows the SM and LQ predictions for the branching fractions $\mathcal{B}$ and LFU ratios R of $B\to D^{(*)}\tau\bar{\nu}$, $B_c\to\eta_c\tau\bar{\nu}$, $B_c\to J/\psi\tau\bar{\nu}$, and $\Lambda_b\to\Lambda_c\tau\bar{\nu}$ decays. The LQ predictions include the uncertainties induced by the transition form factors and CKM matrix elements. Considering that the polarization fractions P_L^{τ} and $P_L^{D^*}$ have already been measured, their SM and LQ predictions are also shown in Table 2. Although the LQ predictions for the branching fractions $\mathcal{B}$ and the LFU ratios R of the $B_c\to\eta_c\tau\bar{\nu}$ and $B_c\to J/\psi\tau\bar{\nu}$ decays lie within the 1σ range of their respective SM values, they can be significantly enhanced by LQ effects.

We set out to analyze the q^2 distributions of the branching fraction $\mathcal{B}$, LFU ratio R, polarization fractions

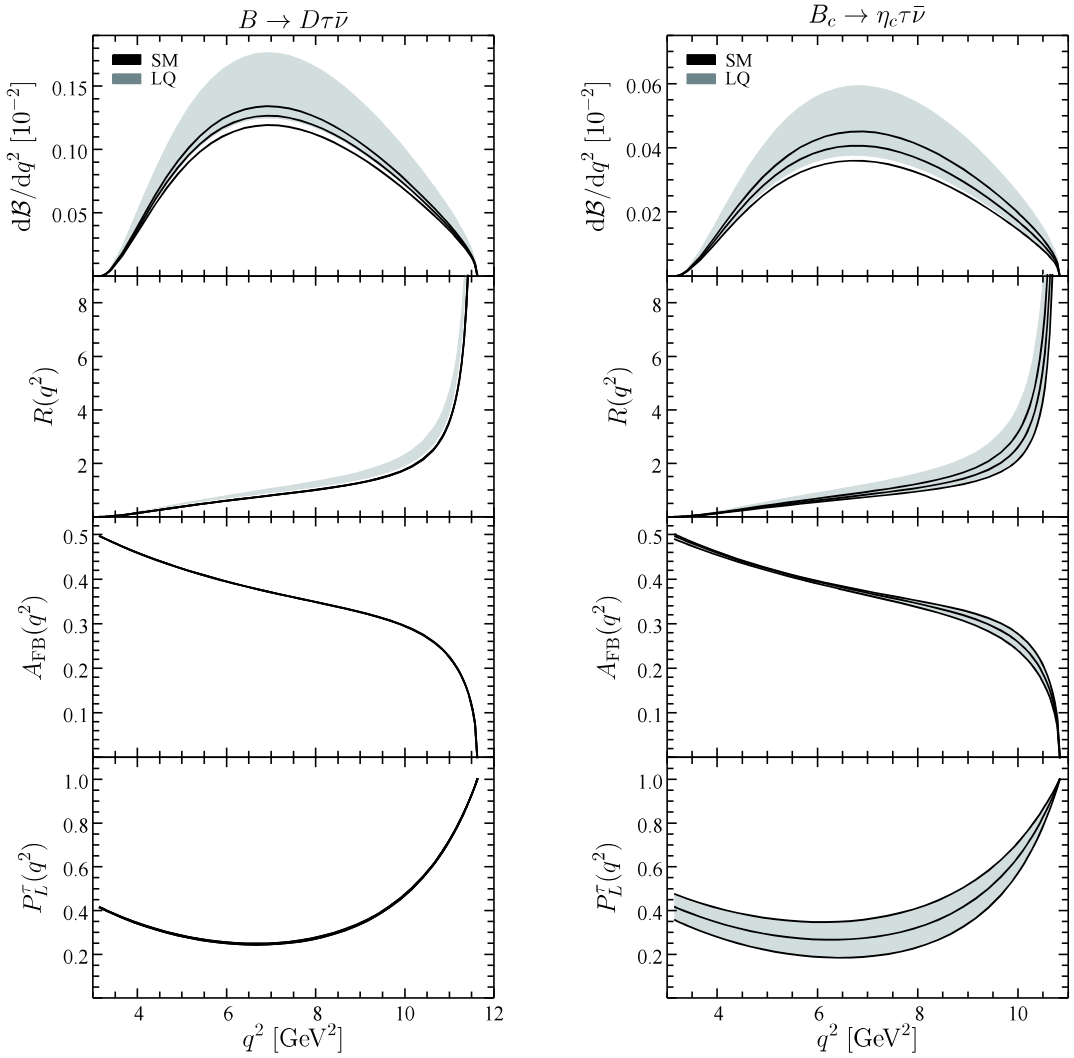

Fig. 3. (color online) q^2 distributions of observables in $B\to D\tau\bar{\nu}$ (left) and $B_c\to\eta_c\tau\bar{\nu}$ (right) decays. The black curves (gray band) indicate the SM (LQ) central values with 1σ theoretical uncertainty.

of the τ lepton (P_L^τ), and daughter hadron ($P_{L,T}^{D^*}$, $P_{L,T}^{J/\psi}$, $P_L^{\Lambda_c}$), as well as the lepton forward-backward asymmetry $A_{\rm FB}$. The $B\to D\tau\nu$ and $B_c\to\eta_c\tau\bar{\nu}$ decays, both part of the "$B\to P$" transition, have differential observables in the SM and the LQ scenario as shown in Fig. 3. All differential observables of the $B\to D\tau\bar{\nu}$ and $B_c\to\eta_c\tau\bar{\nu}$ decays are similar to each other, while the observables in the latter have larger theoretical uncertainties due to the less precise $B_c\to\eta_c$ transition form factors. Therefore, the $B\to D\tau\bar{\nu}$ decay is more sensitive to the LQ effects, with the differential branching fraction largely enhanced, especially near $q^2\sim 7\,{\rm GeV}^2$. The large difference between the SM and LQ predictions in this kinematic region could, therefore, provide a testable signature of the LQ effects. More interestingly, the q^2 distribution of the ratio R in the LQ model is enhanced in the entire kinematic region and does not have overlap with the 1σ SM range. In the future, more precise measurements of these distributions are of importance to confirm the existence of a possible NP effect in the $B\to D\tau\bar{\nu}$ decay. With regard to the forward-backward asymmetry $A_{\rm FB}$ and the τ-lepton polarization fraction P_L^τ in both $B\to D\tau\bar{\nu}$ and $B_c\to\eta_c\tau\bar{\nu}$ decays, the LQ predictions are indistinguishable from the ones in SM, because the LQ effects only modify the Wilson coefficient $C_L^{\ell\nu_\ell}$, which is canceled out exactly in the definitions of these observables (see Eqs. (16) and (17),Fig. 3). This feature is different from the NP scenarios that use scalar or tensor operators to explain the $R_{D^{(*)}}$ anomaly [58–60].

The q^2 distributions of the observables in $B\to D^*\tau\bar{\nu}$ and $B_c\to J/\psi\tau\bar{\nu}$ decays are shown in Fig. 4. Because both of these two decays belong to "$B\to V$" transition, their differential observables are similar. While the differential branching fractions of these two decays are enhanced in the LQ model, their theoretical uncertainties are larger than the ones in the $B\to D\tau\bar{\nu}$ decay. For the q^2 distributions of the ratios R_{D^*} and $R_{J/\psi}$, they are largely enhanced in the entire kinematic region, especially in the large q^2 region. More importantly, although the ranges of the q^2-integrated ratio $R_{D^*,J/\psi}$ in the SM and the LQ scenario overlap at the 1σ level, the 1σ ranges of the differential ratio $R_{D^*,J/\psi}(q^2)$ at large q^2 in the SM and LQ exhiibt significant differences. The increases of R_{D^*} and $R_{J/\psi}$ in the large q^2 region are larger than the one observed in R_D. Measurements of the differential ratios in the large dilepton invariant mass region are, therefore, crucial to confirm the $R_{D^{(*)}}$ anomaly and test the LQ model considered. Similarly to the ones in $B\to D\tau\bar{\nu}$ and $B_c\to\eta_c\tau\bar{\nu}$ decays, the angular distributions $A_{\rm FB}$, $P_{L,T}^{D^*,J/\psi}$, and P_L^τ are likewise not affected by the LQ effects, as shown in Fig. 4.

For the $\Lambda_b\to\Lambda_c\tau\bar{\nu}$ decay, the q^2 distributions of the observables are shown in Fig. 5. The situation is similar in the $B\to D^*\tau\bar{\nu}$ and $B_c\to J/\psi\tau\bar{\nu}$ decays. The q^2 distributions of the branching fraction $\mathcal{B}$ and the ratio R_{Λ_c} are greatly enhanced by the LQ effects. In the large q^2 region, the differential ratio R_{Λ_c} exhibits a deviation between the 1σ permitted ranges of the SM and the LQ scenario. With the large numbers of Λ_b obtained at the HL-LHC [78], we expect that this prediction could provide helpful information on the LQ effects. For the angular distributions, the LQ effects vanish due to the same reason as in the mesonic decays.

5 Conclusions

During the past few years, intriguing hints pointing towards an LFU violation have emerged in the $B\to D^{(*)}\tau\bar{\nu}$ data. Motivated by the recent measurements of $R_{J/\psi}$, P_L^τ, and $P_L^{D^*}$, we revisited the LQ model proposed in Ref. [56], where two scalar LQs, one of which is a $SU(2)_L$ singlet, whereas the other is a $SU(2)_L$ triplet, are introduced simultaneously. Taking into account the recent progress on the transition form factors and the most recent experimental data, we obtained constraints on the LQ couplings λ_{23}^L and λ_{33}^L. Subsequently, we systematically investigated the LQ effects on the five $b\to c\tau\bar{\nu}$ decays, $B\to D^{(*)}\tau\bar{\nu}$, $B_c\to\eta_c\tau\bar{\nu}$, $B_c\to J/\psi\tau\bar{\nu}$, and $\Lambda_b\to\Lambda_c\tau\bar{\nu}$. In particular, we focused on the q^2 distributions of the branching fractions, LFU ratios, and various angular observables. The main results of this study can be summarized as follows:

• After considering the R_D and R_{D^*} data, we obtain the bound on the LQ couplings, $0.03<\lambda_{23}^{L^*}\lambda_{33}^L<0.20$, at the 2σ level. The current measurements of $R_{J/\psi}$, P_L^τ and $P_L^{D^*}$ cannot provide further constraints on the LQ couplings.

• The $B_s\to\tau^+\tau^-$ decay is strongly correlated with $B\to D^{(*)}\tau\bar{\nu}$. To reproduce the 2σ experimental range of $R_{D^{(*)}}$, the LQ effects enhance $\mathcal{B}(B_s\to\tau^+\tau^-)$ by about 2–3 orders of magnitude compared to the SM prediction and hence reach the expected sensitivity of the LHCb Upgrade II.

• The differential branching fractions and LFU ratios are largely enhanced by the LQ effects. Due to their small theoretical uncertainties, the latter provide testable signatures of the LQ model considered, especially in the large dilepton invariant mass squared region. Moreover, R_{Λ_c} in the baryonic decay $\Lambda_b\to\Lambda_c\tau\bar{\nu}$ has the potential to shed new light on the $R_{D^{(*)}}$ anomalies.

• Because no new operators are generated by the LQ effects, all angular distributions in the LQ model are the same as in the SM. We provide the most recent SM predictions for the τ-lepton forward-backward asymmetry, the τ, and meson polarization fractions of the five $b\to c\tau\bar{\nu}$ modes. Although precision measurements of these angular distributions are very challenging at the HL-LHC and SuperKEKB, they are crucial for the veri-

fication of the LQ scenario investigated in this work.

The q^2 distributions of the branching fractions, the LFU ratios, and the various angular observables in $b \to c\tau\bar{\nu}$ transitions can help to confirm possible NP resolutions of the $R_{D^{(*)}}$ anomalies and distinguish among the various NP candidates. With the experimental progress expected from the SuperKEKB [54] and the future HL-LHC [78], our predictions for these observables can be further probed in the near future.

Note Added. After the completion of this work, the Belle Collaboration announced their results of R_D and R_{D^*} with a semileptonic tagging method [105,106]. The measured values are $R_D^{\rm exp} = 0.307 \pm 0.037\,({\rm stat.}) \pm 0.016\,({\rm syst.})$ and $R_{D^*}^{\rm exp} = 0.283 \pm 0.018\,({\rm stat.}) \pm 0.014\,({\rm syst.})$. After includ-

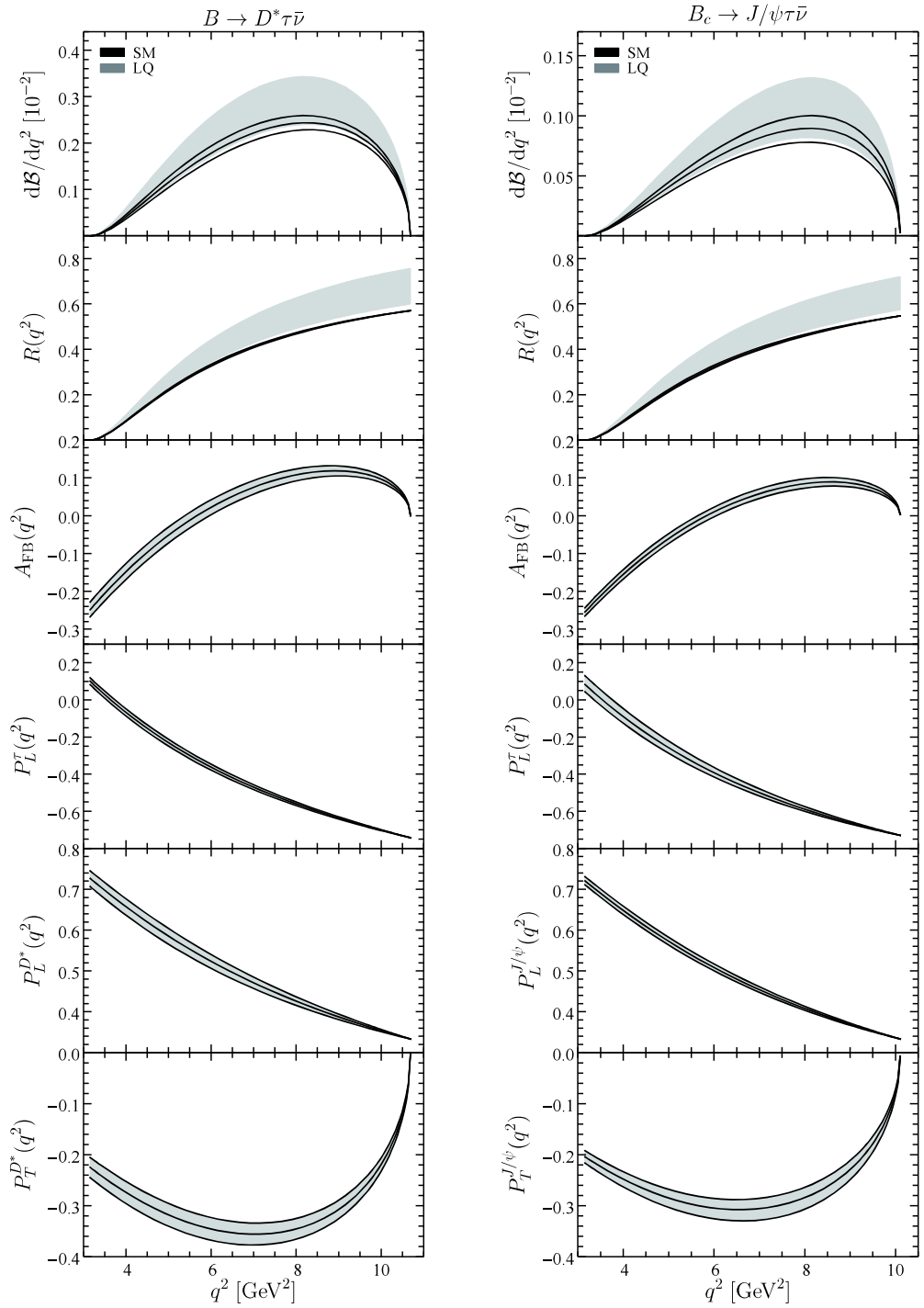

Fig. 4. (color online) q^2 distributions of observables in $B \to D^*\tau\bar{\nu}$ (left) and $B_c \to J/\psi\tau\bar{\nu}$ (right) decays. Other captions are the same as in Fig. 3.

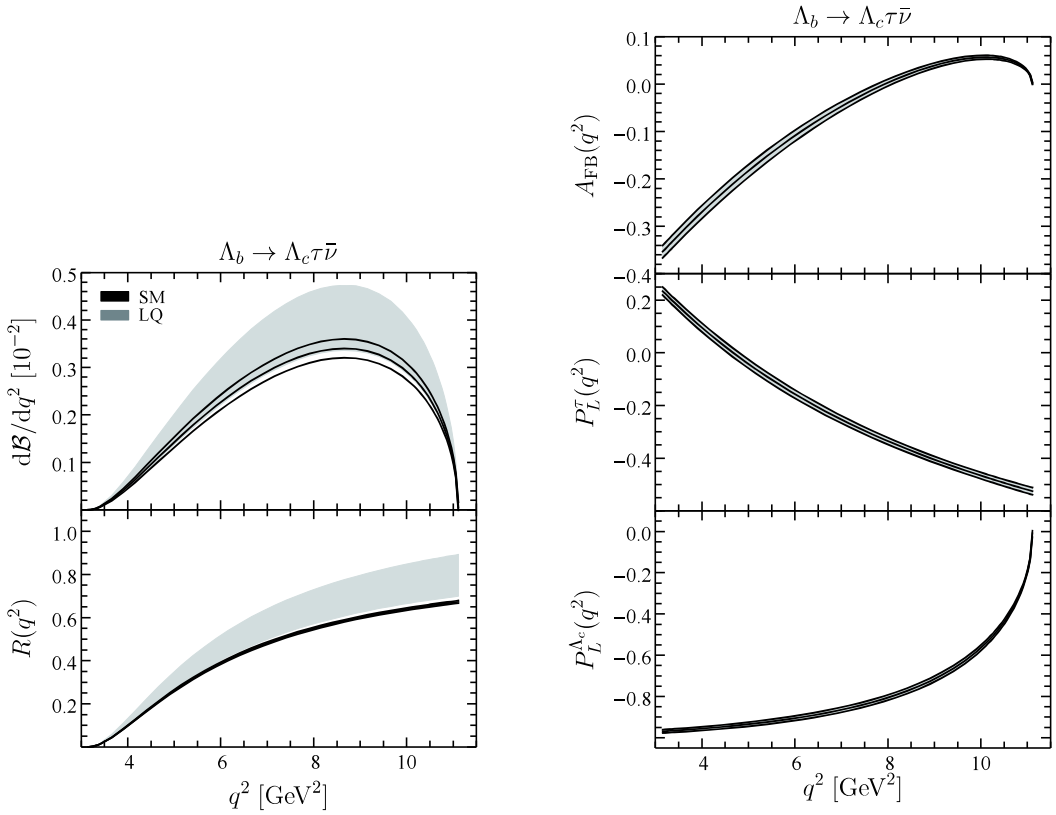

Fig. 5. (color online) q^2 distributions of observables in $\Lambda_b \to \Lambda_c \tau \bar{\nu}$ decay. Other captions are the same as in Fig. 3.

ing this new measurement, the world averages become $R_D^{\rm avg,2019} = 0.337 \pm 0.030$ and $R_{D^*}^{\rm avg,2019} = 0.299 \pm 0.013$ [107]. The deviation of the current world averages from the SM predictions decreases from 3.8σ to 3.1σ [105]. Because the difference between the new and previous averages is small, our numerical results are expected to remain qualitatively unchanged. For example, the updated bounds on $\lambda_{23}^{L*}\lambda_{33}^{L}$ in Eq. (23) becomes $-2.88 < \lambda_{23}^{L*}\lambda_{33}^{L} < -2.73$ and $0.02 < \lambda_{23}^{L*}\lambda_{33}^{L} < 0.17$.

We thank Xin-Qiang Li for useful discussions.

Appendix A: Helicity amplitudes in $b \to c\tau\bar{\nu}$ decays

In the presence of NP, the most general effective Hamiltonian for the $b \to c\tau\bar{\nu}$ transition can be written as [23, 76]

$$\begin{aligned}\mathcal{H}_{\rm eff} =& 2\sqrt{2}G_F V_{cb}\Big[(1+g_L)(\bar{c}\gamma_\mu P_L b)(\bar{\tau}\gamma^\mu P_L \nu_\tau) + g_R(\bar{c}\gamma_\mu P_R b)(\bar{\tau}\gamma^\mu P_L \nu_\tau)\\ &+ \frac{1}{2}g_S(\bar{c}b)(\bar{\tau}P_L\nu_\tau) + \frac{1}{2}g_P(\bar{c}\gamma_5 b)(\bar{\tau}P_L\nu_\tau)\\ &+ g_T(\bar{c}\sigma^{\mu\nu}P_L b)(\bar{\tau}\sigma_{\mu\nu}P_L\nu_\tau)\Big] + \text{h.c.}.\end{aligned} \tag{A1}$$

In this appendix, for completeness, we consider the most general case of NP and provide the helicity amplitudes in the five $b \to c\tau\bar{\nu}$ decays, $B \to D^{(*)}\tau\bar{\nu}$, $B_c \to \eta_c\tau\bar{\nu}$, $B_c \to J/\psi\tau\bar{\nu}$, and $\Lambda_b \to \Lambda_c\tau\bar{\nu}$. Explicit expressions of the spinors and polarization vectors used to calculate the helicity amplitudes are also presented.

A.1 Kinematic conventions

To calculate the hadronic helicity amplitudes of $M \to N\tau\bar{\nu}$ in Eq. (13), we work in the M rest frame and follow the notation of Ref. [79]:

$$p_M^\mu = (m_M, 0, 0, 0), \quad p_N^\mu = (E_N, 0, 0, |\vec{p}_N|), \quad q^\mu = (q_0, 0, 0, -|\vec{q}|), \tag{A2}$$

where q^μ is the four-momentum of the virtual vector boson in the M rest frame, and

$$\begin{aligned}q_0 &= \frac{1}{2m_M}(m_M^2 - m_N^2 + q^2), \quad E_N = \frac{1}{2m_M}(m_M^2 + m_N^2 - q^2),\\ |\vec{q}| &= |\vec{p}_N| = \frac{1}{2m_M}\sqrt{Q_+Q_-}, \quad Q_\pm = (m_M \pm m_N)^2 - q^2.\end{aligned} \tag{A3}$$

Subsequently, substituting the momentum into Eq. (A12), the Dirac spinors in the $\Lambda_b \to \Lambda_c\tau\nu_\tau$ decay can be written as

$$\begin{aligned}u_{\Lambda_b}(\vec{p}_{\Lambda_b}, \lambda_{\Lambda_b}) &= \sqrt{2m_{\Lambda_b}}\begin{pmatrix}\chi(\vec{p}_{\Lambda_b}, \lambda_{\Lambda_b})\\ 0\end{pmatrix},\\ u_{\Lambda_c}(\vec{p}_{\Lambda_c}, \lambda_{\Lambda_c}) &= \begin{pmatrix}\sqrt{E+m_{\Lambda_c}}\chi(\vec{p}_{\Lambda_c}, \lambda_{\Lambda_c})\\ 2\lambda_{\Lambda_c}\sqrt{E-m_{\Lambda_c}}\chi(\vec{p}_{\Lambda_c}, \lambda_{\Lambda_c})\end{pmatrix},\end{aligned} \tag{A4}$$

where $\chi(\vec{p}_{\Lambda_b}, 1/2) = \chi(\vec{p}_{\Lambda_c}, 1/2) = (1,0)^T, \chi(\vec{p}_{\Lambda_b}, -1/2) = \chi(\vec{p}_{\Lambda_c}, -1/2) = (0,1)^T$.

In the $B\to D^*\tau\bar{\nu}$ decay, the polarization vectors of the D^* meson are given by

$$\epsilon^\mu(\vec{p}_{D^*},0)=\frac{1}{m_{D^*}}(|\vec{p}_{D^*}|,0,0,E_{D^*}),\quad \epsilon^\mu(\vec{p}_{D^*},\pm)=\frac{1}{\sqrt{2}}(0,\pm1,i,0). \tag{A5}$$

In all the five $b\to c\tau\bar{\nu}$ decays, the polarization vectors for the virtual vector boson W can be written as

$$\epsilon^\mu(t)=\frac{1}{\sqrt{q^2}}(q_0,0,0,-|\vec{q}|),\quad \epsilon^\mu(0)=\frac{1}{\sqrt{q^2}}(|\vec{q}|,0,0,-q_0),$$
$$\epsilon^\mu(\pm)=\frac{1}{\sqrt{2}}(0,\mp1,i,0), \tag{A6}$$

and the orthonormality and completeness relation [108]

$$\sum_\mu \epsilon^*_\mu(m)\epsilon^\mu(n)=g_{mn},\quad \sum_{m,n}\epsilon_\mu(m)\epsilon^*_\nu(n)g_{mn}=g_{\mu\nu},\quad m,n\in\{t,\pm,0\}, \tag{A7}$$

where $g_{mn}=\mathrm{diag}(+1,-1,-1,-1)$.

In the calculation of the leptonic helicity amplitudes, we work in the rest frame of the virtual vector boson W, which is equivalent to the rest frame of the τ-$\bar{\nu}_\tau$ system. Following Ref. [79], we have

$$q^\mu=(\sqrt{q^2},0,0,0),\quad p^\mu_\tau=(E_\tau,|\vec{p}_\tau|\sin\theta_\tau,0,|\vec{p}_\tau|\cos\theta_\tau),$$
$$p^\mu_{\bar{\nu}}=|\vec{p}_\tau|(1,-\sin\theta_\tau,0,-\cos\theta_\tau), \tag{A8}$$

where $|\vec{p}_\tau|=\sqrt{q^2}v^2/2$, $E_\tau=|\vec{p}_\tau|+m_\tau^2/\sqrt{q^2}$, $v=\sqrt{1-m_\tau^2/q^2}$, and θ_τ denotes the angle between the three-momenta of the τ and the N.

The Dirac spinors for τ and $\bar{\nu}_\tau$ read

$$u_\tau(\vec{p}_\tau,\lambda_\tau)=\begin{pmatrix}\sqrt{E_\tau+m_\tau}\chi(\vec{p}_\tau,\lambda_\tau)\\ 2\lambda_\tau\sqrt{E_\tau-m_\tau}\chi(\vec{p}_\tau,\lambda_\tau)\end{pmatrix},$$
$$v_{\bar{\nu}_\tau}(-\vec{p}_\tau,\tfrac{1}{2})=\sqrt{E_\nu}\begin{pmatrix}\xi(-\vec{p}_\tau,\frac{1}{2})\\ -\xi(-\vec{p}_\tau,\frac{1}{2})\end{pmatrix}, \tag{A9}$$

respectively. Further details are given in Appendix A.2

The polarization vectors of the virtual vector boson in the W rest frame are written as

$$\bar{\epsilon}^\mu(t)=(1,0,0,0),\quad \bar{\epsilon}^\mu(0)=(0,0,0,-1),\quad \bar{\epsilon}^\mu(\pm)=\frac{1}{\sqrt{2}}(0,\mp1,i,0), \tag{A10}$$

which can also be obtained from Eq. (A6) by a Lorentz transformation and satisfy the orthonormality and completeness relation in Eq. (A7).

A.2 Dirac spinor

The definitions of the helicity operator $h_{\vec{p}}$ and its eigenstates are given as follows [109]

$$h_{\vec{p}}\equiv\frac{1}{2}\hat{\vec{p}}\cdot\vec{\sigma},\quad \hat{\vec{p}}\equiv\frac{\vec{p}}{|\vec{p}|},\quad h_{\vec{p}}\,\chi(\vec{p},s)=s\,\chi(\vec{p},s),$$

where $\vec{p}$ denotes the momentum of the particle, and $\vec{\sigma}=\{\sigma^1,\sigma^2,\sigma^3\}$ are the Pauli matrices. Eigenstates of the helicity operator $h_{\vec{p}}$ read

$$\chi\left(\vec{p},\frac{1}{2}\right)=\begin{pmatrix}\cos\frac{\theta}{2}\\ e^{i\phi}\sin\frac{\theta}{2}\end{pmatrix},\quad \chi\left(\vec{p},-\frac{1}{2}\right)=\begin{pmatrix}-e^{-i\phi}\sin\frac{\theta}{2}\\ \cos\frac{\theta}{2}\end{pmatrix},$$
$$\chi\left(-\vec{p},\frac{1}{2}\right)=\begin{pmatrix}\sin\frac{\theta}{2}\\ -e^{i\phi}\cos\frac{\theta}{2}\end{pmatrix},\quad \chi\left(-\vec{p},-\frac{1}{2}\right)=\begin{pmatrix}e^{-i\phi}\cos\frac{\theta}{2}\\ \sin\frac{\theta}{2}\end{pmatrix}, \tag{A11}$$

for the normalized momentum $\hat{\vec{p}}=\{\sin\theta\cos\phi,\sin\theta\sin\phi,\cos\theta\}$.

Using these eigenstates, the solution of Dirac equation $(\gamma^\mu p_\mu-m)u(\vec{p},s)=0$ in Dirac representation can be written as

$$u(\vec{p},s)=\begin{pmatrix}\sqrt{E+m}\,\chi(\vec{p},s)\\ 2s\sqrt{E-m}\,\chi(\vec{p},s)\end{pmatrix}. \tag{A12}$$

Further, the spinor for the antiparticle can be obtained by $v(\vec{p},s)\equiv C\bar{u}(\vec{p},s)^T=i\gamma^0\gamma^2\bar{u}(\vec{p},s)^T$[1)], whose explicit expression reads

$$v(\vec{p},s)=\begin{pmatrix}\sqrt{E-m}\,\xi(\vec{p},s)\\ -2s\sqrt{E+m}\,\xi(\vec{p},s)\end{pmatrix}, \tag{A13}$$

where $\xi(\vec{p},s)=\chi(\vec{p},-s)$ and $\xi(\vec{p},s)$ satisfies $h_{\vec{p}}\,\xi(\vec{p},s)=-s\,\xi(\vec{p},s)$.

The spinors in Weyl representation read

$$u_W(\vec{p},s)=\begin{pmatrix}\sqrt{E-2s|\vec{p}|}\,\chi(\vec{p},s)\\ \sqrt{E+2s|\vec{p}|}\,\chi(\vec{p},s)\end{pmatrix},$$
$$v_W(\vec{p},s)=\begin{pmatrix}-2s\sqrt{E+2s|\vec{p}|}\,\xi(\vec{p},s)\\ 2s\sqrt{E-2s|\vec{p}|}\,\xi(\vec{p},s)\end{pmatrix}. \tag{A14}$$

They can also be obtained from the Dirac representation by the relation $u_W(\vec{p},s)=Xu(\vec{p},s)$ with the transformation matrix

$$X=\frac{1}{\sqrt{2}}\begin{pmatrix}1&-1\\1&1\end{pmatrix}.$$

In the τ-$\bar{\nu}_\tau$ center-of-mass frame, we emphasize that if the τ spinor is specified as $u(\vec{p},s)$ in the leptonic helicity amplitude, then the $\bar{\nu}_\tau$ spinor has the form $v(-\vec{p},s)$, as in Eq. (A9). All calculations in our work are depictec in Dirac representation.

A.3 Leptonic helicity amplitudes

The leptonic helicity amplitudes in Eq. (13) are defined as [79]

$$\begin{aligned}L^{SP}_{\lambda_\tau}&=\langle\tau\bar{\nu}_\tau|\bar{\tau}(1-\gamma_5)\nu_\tau|0\rangle=\bar{u}_\tau(\vec{p}_\tau,\lambda_\tau)(1-\gamma_5)v_{\bar{\nu}_\tau}(-\vec{p}_\tau,1/2),\\ L^{VA}_{\lambda_\tau,\lambda_W}&=\bar{\epsilon}^\mu(\lambda_W)\langle\tau\bar{\nu}_\tau|\bar{\tau}\gamma_\mu(1-\gamma_5)\nu_\tau|0\rangle\\ &=\bar{\epsilon}^\mu(\lambda_W)\bar{u}_\tau(\vec{p}_\tau,\lambda_\tau)\gamma_\mu(1-\gamma_5)v_{\bar{\nu}_\tau}(-\vec{p}_\tau,1/2),\\ L^{T}_{\lambda_\tau,\lambda_{W_1},\lambda_{W_2}}&=-i\bar{\epsilon}^\mu(\lambda_{W_1})\bar{\epsilon}^\nu(\lambda_{W_2})\langle\tau\bar{\nu}_\tau|\bar{\tau}\sigma_{\mu\nu}(1-\gamma_5)\nu_\tau|0\rangle\\ &=-i\bar{\epsilon}^\mu(\lambda_{W_1})\bar{\epsilon}^\nu(\lambda_{W_2})\bar{u}_\tau(\vec{p}_\tau,\lambda_\tau)\sigma_{\mu\nu}(1-\gamma_5)v_{\bar{\nu}_\tau}(-\vec{p}_\tau,1/2),\end{aligned} \tag{A15}$$

Obtaining $L^T_{\lambda_\tau,\lambda_{W_1},\lambda_{W_2}}=-L^T_{\lambda_\tau,\lambda_{W_2},\lambda_{W_1}}$ is straightforward. The nonzero leptonic helicity amplitudes read

$$\begin{aligned}L^{SP}_{1/2}&=2\sqrt{q^2}v,\\ L^{VA}_{1/2,t}&=2m_\tau v,\\ L^{VA}_{1/2,0}&=-2m_\tau v\cos\theta_\tau,\\ L^{VA}_{-1/2,0}&=2\sqrt{q^2}v\sin\theta_\tau,\\ L^{VA}_{1/2,\pm}&=\mp\sqrt{2}m_\tau v\sin\theta_\tau,\\ L^{VA}_{-1/2,\pm}&=\sqrt{2q^2}v(-1\mp\cos\theta_\tau),\\ L^{T}_{1/2,0,\pm}&=\pm L^T_{1/2,\pm,t}=\sqrt{2q^2}v\sin\theta_\tau,\\ L^{T}_{1/2,t,0}&=L^T_{1/2,+,-}=-2\sqrt{q^2}v\cos\theta_\tau,\\ L^{T}_{-1/2,0,\pm}&=\pm L^T_{-1/2,\pm,t}=\sqrt{2}m_\tau v(\pm1+\cos\theta_\tau),\\ L^{T}_{-1/2,t,0}&=L^T_{-1/2,+,-}=2m_\tau v\sin\theta_\tau.\end{aligned} \tag{A16}$$

A.4 Hadronic helicity amplitudes

The hadronic helicity amplitudes $M\to N$ are defined as

1) The selection $C=i\gamma^2\gamma^0$ is also permissible, but the $v(\vec{p},s)$ will have an additional negative sign.

$$
\begin{aligned}
H^{S}_{\lambda_M,\lambda_N} &= \langle N(\lambda_N)|\bar{c}b|M(\lambda_M)\rangle,\\
H^{P}_{\lambda_M,\lambda_N} &= \langle N(\lambda_N)|\bar{c}\gamma_5 b|M(\lambda_M)\rangle,\\
H^{V}_{\lambda_M,\lambda_N,\lambda_W} &= \epsilon^{*}_{\mu}(\lambda_W)\langle N(\lambda_N)|\bar{c}\gamma^{\mu}b|M(\lambda_M)\rangle,\\
H^{A}_{\lambda_M,\lambda_N,\lambda_W} &= \epsilon^{*}_{\mu}(\lambda_W)\langle N(\lambda_N)|\bar{c}\gamma^{\mu}\gamma_5 b|M(\lambda_M)\rangle,\\
H^{T_1,\lambda_M}_{\lambda_N,\lambda_{W_1},\lambda_{W_2}} &= i\epsilon^{*}_{\mu}(\lambda_{W_1})\epsilon^{*}_{\nu}(\lambda_{W_2})\langle N(\lambda_N)|\bar{c}\sigma^{\mu\nu}b|M(\lambda_M)\rangle,\\
H^{T_2,\lambda_M}_{\lambda_N,\lambda_{W_1},\lambda_{W_2}} &= i\epsilon^{*}_{\mu}(\lambda_{W_1})\epsilon^{*}_{\nu}(\lambda_{W_2})\langle N(\lambda_N)|\bar{c}\sigma_{\mu\nu}\gamma_5 b|M(\lambda_M)\rangle,
\end{aligned}
\tag{A17}
$$

and

$$
\begin{aligned}
H^{SP}_{\lambda_M,\lambda_N} &= g_S H^{S}_{\lambda_M,\lambda_N} + g_P H^{P}_{\lambda_M,\lambda_N},\\
H^{VA}_{\lambda_M,\lambda_N,\lambda_W} &= (1+g_L+g_R)H^{V}_{\lambda_N,\lambda_W} - (1+g_L-g_R)H^{A}_{\lambda_M,\lambda_N,\lambda_W},\\
H^{T,\lambda_M}_{\lambda_N,\lambda_{W_1},\lambda_{W_2}} &= g_T H^{T_1,\lambda_M}_{\lambda_N,\lambda_{W_1},\lambda_{W_2}} - g_T H^{T_2,\lambda_M}_{\lambda_N,\lambda_{W_1},\lambda_{W_2}},
\end{aligned}
\tag{A18}
$$

$H^{T,\lambda_M}_{\lambda_N,\lambda_{W_1},\lambda_{W_2}} = -H^{T,\lambda_M}_{\lambda_N,\lambda_{W_2},\lambda_{W_1}}$ is easily obtained. The amplitudes $H^{T_1,\lambda_M}_{\lambda_N,\lambda_{W_1},\lambda_{W_2}}$ and $H^{T_2,\lambda_M}_{\lambda_N,\lambda_{W_1},\lambda_{W_2}}$ are connected by the relation $\sigma_{\mu\nu}\gamma_5 = -(i/2)\epsilon^{\mu\nu\alpha\beta}\sigma_{\alpha\beta}$, where $\epsilon^{0123} = -1$.

Appendix B: Form factors

The hadronic matrix elements for the $B \to D$ transition can be parameterized in terms of form factors $F_{+,0,T}$ [110, 111]. In the BGL parametrization, the form factors $F_{+,0}$ can be written as expressions of a^{+}_{n} and a^{0}_{n} [13],

$$
\begin{aligned}
F_{+}(z) &= \frac{1}{P_{+}(z)\phi_{+}(z,\mathcal{N})}\sum_{n=0}^{\infty} a^{+}_{n} z^{n}(w,\mathcal{N}),\\
F_{0}(z) &= \frac{1}{P_{0}(z)\phi_{0}(z,\mathcal{N})}\sum_{n=0}^{\infty} a^{0}_{n} z^{n}(w,\mathcal{N}),
\end{aligned}
\tag{B1}
$$

where $r = m_D/m_B$, $\mathcal{N} = (1+r)/(2\sqrt{r})$, $w = (m_B^2+m_D^2-q^2)/(2m_B m_D)$, $z(w,\mathcal{N}) = (\sqrt{1+w}-\sqrt{2\mathcal{N}})/(\sqrt{1+w}+\sqrt{2\mathcal{N}})$, and $F_{+}(0) = F_{0}(0)$. The values of the fit parameters are taken from Ref. [13]. Expressions of the tensor form factor F_T can be found in Ref. [110].

For $B \to D^{*}$ transition, the relevant form factors $\{V, A_{0,1,2}\}$ can be written in terms of the form factors $\{h_V, h_{A_{1,2,3}}\}$ in the heavy quark effective theory (HQET) [110],

$$
\begin{aligned}
V(q^2) &= \frac{m_{+}}{2\sqrt{m_B m_{D^{*}}}}h_V(w),\\
A_0(q^2) &= \frac{1}{2\sqrt{m_B m_{D^{*}}}}\left[\frac{m_{+}^2-q^2}{2m_{D^{*}}}h_{A_1}(w) - \frac{m_{+}m_{-}+q^2}{2m_B}h_{A_2}(w) - \frac{m_{+}m q^2}{2m_{D^{*}}}h_{A_3}(w)\right],\\
A_1(q^2) &= \frac{m_{+}^2-q^2}{2\sqrt{m_B m_{D^{*}}}m_{+}}h_{A_1}(w),\\
A_2(q^2) &= \frac{m_{+}}{2\sqrt{m_B m_{D^{*}}}}\left[h_{A_3}(w) + \frac{m_{D^{*}}}{m_B}h_{A_2}(w)\right],
\end{aligned}
\tag{B2}
$$

where $m_{\pm} = m_B \pm m_{D^{*}}$ and $w = (m_B^2+m_{D^{*}}^2-q^2)/2m_B m_{D^{*}}$. In the CLN parametrization, the HQET form factors can be expressed as [89]

$$
\frac{h_V(w)}{h_{A_1}(w)} = R_1(w), \quad \frac{h_{A_2}(w)}{h_{A_1}(w)} = \frac{R_2(w)-R_3(w)}{2r_{D^{*}}},
$$

$$
\frac{h_{A_3}(w)}{h_{A_1}(w)} = \frac{R_2(w)+R_3(w)}{2},
\tag{B3}
$$

with $r = m_{D^{*}}/m_B$. Numerically we obtain,

$$
\begin{aligned}
h_{A_1}(w) &= h_{A_1}(1)[1-8\rho^2_{D^{*}}z + (53\rho^2_{D^{*}}-15)z^2 - (231\rho^2_{D^{*}}-91)z^3],\\
R_1(w) &= R_1(1) - 0.12(w-1) + 0.05(w-1)^2,\\
R_2(w) &= R_2(1) + 0.11(w-1) - 0.06(w-1)^2,\\
R_3(w) &= 1.22 - 0.052(w-1) + 0.026(w-1)^2,
\end{aligned}
\tag{B4}
$$

with $z = (\sqrt{w+1}-\sqrt{2})/(\sqrt{w+1}+\sqrt{2})$. The fit parameters $R_1(1)$, $R_2(1)$, $h_{A_1}(1)$ and $\rho^2_{D^{*}}$ are taken from Ref. [14]. Expressions of the tensor form factors $T_{1,2,3}$ can be found in Ref. [110].

The $\Lambda_b \to \Lambda_c$ hadronic matrix elements can be written in terms of ten helicity form factors $\{F_{0,+,\perp}, G_{0,+,\perp}, h_{+,\perp}, \widetilde{h}_{+,\perp}\}$ [75, 76]. Following Ref. [75], the lattice calculations are fitted to two (Bourrely-Caprini-Lellouch) BCL z-parametrizations. In the so called "nominal" fit, a form factor f reduces to the form

$$
f(q^2) = \frac{1}{1-q^2/(m^{f}_{\rm pole})^2}[a^{f}_{0} + a^{f}_{1}z^{f}(q^2)],
\tag{B5}
$$

while a form factor f in the higher-order fit is given by

$$
\begin{aligned}
f_{\rm HO}(q^2) = \frac{1}{1-q^2/(m^{f}_{\rm pole})^2}\{&a^{f}_{0,\rm HO} + a^{f}_{1,\rm HO}z^{f}(q^2)\\
&+ a^{f}_{2,\rm HO}[z^{f}(q^2)]^2\},
\end{aligned}
\tag{B6}
$$

where $t_0 = (m_{\Lambda_b}-m_{\Lambda_c})^2$, $t^{f}_{+} = (m^{f}_{\rm pole})^2$, and $z^{f}(q^2) = \left|\left(\sqrt{t^{f}_{+}-q^2}-\sqrt{t^{f}_{+}-t_0}\right)\right/\left(\sqrt{t^{f}_{+}-q^2}+\sqrt{t^{f}_{+}-t_0}\right)\right|$. The values of the fit parameters and all the pole masses are taken from Ref. [76].

In addition, the form factors for $B_c \to J/\psi\ell\bar{\nu}_\ell$ and $B_c \to \eta_c\ell\bar{\nu}_\ell$ decays are taken form the results in the Covariant Light-Front Approach in Ref. [18].

Appendix C: Observables in $b \to c\tau\bar{\nu}$ decays

C.1 $B \to D\tau\bar{\nu}$ and $B_c \to \eta_c\tau\bar{\nu}$ decays

Because similar expressions hold for the $B \to D\tau\bar{\nu}$ and $B_c \to \eta_c\tau\bar{\nu}$ decays, we only provide the theoretical formulae of the former. Using the form factors in Appendix B, the non-zero helicity amplitudes for the $B \to D\tau\bar{\nu}$ decay in Eq. (A18) can be written as

$$
\begin{aligned}
H^{VA}_{0}(q^2) &= (1+g_{\rm L}+g_{\rm R})\sqrt{\frac{Q_{+}Q_{-}}{q^2}}F_{+}(q^2),\\
H^{VA}_{t}(q^2) &= (1+g_{\rm L}+g_{\rm R})\frac{m_B^2-m_D^2}{\sqrt{q^2}}F_0(q^2),\\
H^{SP}(q^2) &= g_S\frac{m_B^2-m_D^2}{m_b-m_c}F_0(q^2),\\
H^{T}_{-,+}(q^2) &= H^{T}_{t,0}(q^2) = g_T\frac{\sqrt{Q_{+}Q_{-}}}{m_B+m_D}F_T(q^2).
\end{aligned}
\tag{C1}
$$

Subsequently, the differential decay width in Eq. (11) and angular observables in Eq. (16) and (17) are obtained

$$\frac{\mathrm{d}\Gamma}{\mathrm{d}q^2} = \frac{N_D}{2}\Big[\frac{3m_\tau^2}{q^2}|H_t^{VA}|^2 + \Big(2+\frac{m_\tau^2}{q^2}\Big)|H_0^{VA}|^2 + 3|H^{SP}|^2 + 16\Big(1+\frac{2m_\tau^2}{q^2}\Big) \times |H_{t,0}^T|^2 + \frac{6m_\tau}{\sqrt{q^2}}\Re[H^{SP}H_t^{VA*}] + \frac{24m_\tau}{\sqrt{q^2}}\Re[H_{t,0}^T H_0^{VA*}]\Big], \tag{C2}$$

$$\frac{\mathrm{d}A_{\rm FB}}{\mathrm{d}q^2} = \frac{3N_D}{2}\Re\Big[\Big(4H_{t,0}^{T*} + \frac{m_\tau}{\sqrt{q^2}}H_0^{VA*}\Big)\Big(H^{SP} + \frac{m_\tau}{\sqrt{q^2}}H_t^{VA}\Big)\Big], \tag{C3}$$

$$\frac{\mathrm{d}P_L^\tau}{\mathrm{d}q^2} = \frac{1}{\mathrm{d}\Gamma/\mathrm{d}q^2}\frac{N_D}{2}\Big[\frac{3m_\tau^2}{q^2}|H_t^{VA}|^2 + \Big(\frac{m_\tau^2}{q^2}-2\Big)|H_0^{VA}|^2 + 3|H^{SP}|^2 + 16\Big(1-\frac{2m_\tau^2}{q^2}\Big)|H_{t,0}^T|^2 + \frac{6m_\tau}{\sqrt{q^2}}\Re[H^{SP}H_t^{VA*}] - \frac{8m_\tau}{\sqrt{q^2}}\Re[H_{t,0}^T H_0^{VA*}]\Big], \tag{C4}$$

with

$$N_D = \frac{G_F^2|V_{cb}|^2}{192\pi^3}\frac{q^2\sqrt{Q_+Q_-}}{m_B^3}\Big(1-\frac{m_\tau^2}{q^2}\Big)^2. \tag{C5}$$

C.2 $B\to D^*\tau\bar{\nu}$ and $B_c\to J/\psi\tau\bar{\nu}$ decays

Because similar expressions hold for the $B\to D^*\tau\bar{\nu}$ and $B_c\to J/\psi\tau\bar{\nu}$ decays, only theoretical formulae of the former are provided in this subsection. Using the form factors in Appendix B, the non-zero helicity amplitudes for the $B\to D^*\tau\bar{\nu}$ decay in Eq. (A18) can be written as

$$\begin{aligned}
H_0^{SP}(q^2) &= -g_P\frac{\sqrt{Q_+Q_-}}{m_b+m_c}A_0(q^2),\\
H_{\pm,\pm}^{VA}(q^2) &= -(1+g_L-g_R)m_+A_1(q^2) \pm (1+g_L+g_R)\frac{\sqrt{Q_+Q_-}}{m_+}V(q^2),\\
H_{0,t}^{VA}(q^2) &= -(1+g_L-g_R)\frac{\sqrt{Q_+Q_-}}{\sqrt{q^2}}A_0(q^2),\\
H_{0,0}^{VA}(q^2) &= \frac{(1+g_L-g_R)}{2m_{D^*}\sqrt{q^2}}\Big[-m_+(m_+m_- - q^2)A_1(q^2) + \frac{Q_+Q_-}{m_+}A_2(q^2)\Big],\\
H_{\pm,\pm,t}^T(q^2) &= \pm H_{\pm,\pm,0}^T(q^2) = \frac{g_T}{\sqrt{q^2}}\Big[\mp\sqrt{Q_+Q_-}T_1(q^2) - m_+m_-T_2(q^2)\Big],\\
H_{0,t,0}^T(q^2) &= H_{0,-,+}^T(q^2) = \frac{g_T}{2m_{D^*}}\Big[-(m_B^2+3m_{D^*}^2-q^2)T_2(q^2) + \frac{Q_+Q_-}{m_+m_-}T_3(q^2)\Big],
\end{aligned} \tag{C6}$$

with $m_\pm = m_B \pm m_{D^*}$. Then, the differential decay width in Eq. (11) and the angular observables in Eq. (16) and (17) are obtained, respectively, as

$$\frac{\mathrm{d}\Gamma}{\mathrm{d}q^2} = N_{D^*}\Big[\frac{3m_\tau^2}{2q^2}|H_{0,t}^{VA}|^2 + \Big(1+\frac{m_\tau^2}{2q^2}\Big)(|H_{-,-}^{VA}|^2 + |H_{0,0}^{VA}|^2 + |H_{+,+}^{VA}|^2) + \frac{3}{2}|H_0^{SP}|^2 + 8\Big(1+\frac{2m_\tau^2}{q^2}\Big)(|H_{0,t,0}^T|^2 + |H_{+,+,t}^T|^2 + |H_{-,-,t}^T|^2) + \frac{3m_\tau}{\sqrt{q^2}}\Re[H_0^{SP}H_{0,t}^{VA*}] + \frac{12m_\tau}{\sqrt{q^2}}(\Re[H_{0,t,0}^T H_{0,0}^{VA*} - H_{+,+,t}^T H_{+,+}^{VA*} - H_{-,-,t}^T H_{-,-}^{VA*}])\Big], \tag{C7}$$

$$\frac{\mathrm{d}A_{\rm FB}}{\mathrm{d}q^2} = \frac{3N_{D^*}}{4}\Big[\frac{2m_\tau^2}{q^2}\Re[H_{0,0}^{VA}H_{0,t}^{VA*}] - |H_{-,-}^{VA}|^2 + |H_{+,+}^{VA}|^2 + 8\Re[H_0^{SP}H_{0,t,0}^{T*}] + \frac{16m_\tau^2}{q^2}(|H_{+,+,t}^T|^2 - |H_{-,-,t}^T|^2) + \frac{2m_\tau}{\sqrt{q^2}}\Re[H_0^{SP}H_{0,0}^{VA*}] + \frac{8m_\tau}{\sqrt{q^2}}\Re[H_{0,t,0}^T H_{0,t}^{VA*} + H_{-,-,t}^T H_{-,-}^{VA*} - H_{+,+,t}^T H_{+,+}^{VA*}]\Big], \tag{C8}$$

$$\frac{\mathrm{d}P_L^{D^*}}{\mathrm{d}q^2} = \frac{1}{\mathrm{d}\Gamma/\mathrm{d}q^2}\frac{N_{D^*}}{2}\Big[\frac{3m_\tau^2}{q^2}|H_{0,t}^{VA}|^2 + \Big(2+\frac{m_\tau^2}{q^2}\Big)|H_{0,0}^{VA}|^2 + 3|H_0^{SP}|^2 + 16\Big(1+\frac{2m_\tau^2}{q^2}\Big)|H_{0,t,0}^T|^2 + \frac{6m_\tau}{\sqrt{q^2}}\Re[H_0^{SP}H_{0,t}^{VA*}] + \frac{24m_\tau}{\sqrt{q^2}}\Re[H_{0,t,0}^T H_{0,0}^{VA*}]\Big], \tag{C9}$$

$$\frac{\mathrm{d}P_L^\tau}{\mathrm{d}q^2} = \frac{1}{\mathrm{d}\Gamma/\mathrm{d}q^2}\frac{N_{D^*}}{2}\Big[\frac{3m_\tau^2}{q^2}|H_{0,t}^{VA}|^2 + \Big(\frac{m_\tau^2}{q^2}-2\Big)(|H_{+,+}^{VA}|^2 + |H_{0,0}^{VA}|^2 + |H_{-,-}^{VA}|^2) + 3|H_0^{SP}|^2 + \frac{6m_\tau}{\sqrt{q^2}}\Re[H_0^{SP}H_{0,t}^{VA*}] + 16\Big(1-\frac{2m_\tau^2}{q^2}\Big)(|H_{0,t,0}^T|^2 + |H_{-,-,t}^T|^2 + |H_{+,+,t}^T|^2) + \frac{8m_\tau}{\sqrt{q^2}}\Re[H_{-,-,t}^T H_{-,-}^{VA*} + H_{+,+,t}^T H_{+,+}^{VA*} - H_{0,t,0}^T H_{0,0}^{VA*}]\Big], \tag{C10}$$

$$\frac{\mathrm{d}P_T^{D^*}}{\mathrm{d}q^2} = \frac{1}{\mathrm{d}\Gamma/\mathrm{d}q^2}\frac{N_{D^*}}{2}\Big[\Big(2+\frac{m_\tau^2}{q^2}\Big)(|H_{+,+}^{VA}|^2 - |H_{-,-}^{VA}|^2) + 16(1+\frac{2m_\tau^2}{q^2})(|H_{+,+,t}^T|^2 - |H_{-,-,t}^T|^2) + \frac{24m_\tau}{\sqrt{q^2}}\Re[H_{-,-,t}^T H_{-,-}^{VA*} - H_{+,+,t}^T H_{+,+}^{VA*}]\Big], \tag{C11}$$

with

$$N_{D^*} = \frac{G_F^2|V_{cb}|^2}{192\pi^3}\frac{q^2\sqrt{Q_+Q_-}}{m_B^3}\Big(1-\frac{m_\tau^2}{q^2}\Big)^2. \tag{C12}$$

C.3 $\Lambda_b\to\Lambda_c\tau\bar{\nu}$ decay

Using the transition form factors in Appendix B, the helicity amplitudes for the $\Lambda_b\to\Lambda_c$ decay in Eq. (A18) can be written as

$$\begin{aligned}
H_{\pm1/2,\pm1/2}^{SP} &= F_0 g_S\frac{\sqrt{Q_+}}{m_b-m_c}m_- \mp G_0 g_P\frac{\sqrt{Q_-}}{m_b+m_c}m_+,\\
H_{\pm1/2,\pm1/2,t}^{VA} &= F_0(1+g_L+g_R)\frac{\sqrt{Q_+}}{\sqrt{q^2}}m_- \mp G_0(1+g_L-g_R)\frac{\sqrt{Q_-}}{\sqrt{q^2}}m_+,\\
H_{\pm1/2,\pm1/2,0}^{VA} &= F_+(1+g_L+g_R)\frac{\sqrt{Q_-}}{\sqrt{q^2}}m_+ \mp G_+(1+g_L-g_R)\frac{\sqrt{Q_+}}{\sqrt{q^2}}m_-,\\
H_{\mp1/2,\pm1/2,\pm}^{VA} &= F_\perp(1+g_L+g_R)\sqrt{2Q_-} \mp G_\perp(1+g_L-g_R)\sqrt{2Q_+},\\
H_{\pm1/2,t,0}^{T,\pm1/2} &= H_{\pm1/2,-,+}^{T,\pm1/2} = g_T\Big[h_+\sqrt{Q_-} \pm \widetilde{h}_+\sqrt{Q_+}\Big],\\
H_{\mp1/2,t,\mp}^{T,\pm1/2} &= \mp H_{\mp1/2,0,\mp}^{T,\pm1/2} = g_T\frac{\sqrt{2}}{\sqrt{q^2}}\Big[h_\perp m_+\sqrt{Q_-} \mp \widetilde{h}_\perp m_-\sqrt{Q_+}\Big],
\end{aligned} \tag{C13}$$

with $m_\pm = m_{\Lambda_b} \pm m_{\Lambda_c}$. Thus, the differential decay width in Eq. (11) can be written as

$$\frac{\mathrm{d}\Gamma}{\mathrm{d}q^2} = N_{\Lambda_c}\Big[A_1^{VA} + \frac{m_\tau^2}{2q^2}A_2^{VA} + \frac{3}{2}A_3^{SP} + 8\Big(1+\frac{2m_\tau^2}{q^2}\Big)A_4^T + \frac{3m_\tau}{\sqrt{q^2}}(A_5^{VA-SP} + 4A_6^{VA-T})\Big], \tag{C14}$$

with

$$\begin{aligned}
N_{\Lambda_c} &= \frac{G_F^2|V_{cb}|^2}{384\pi^3}\frac{q^2\sqrt{Q_+Q_-}}{m_{\Lambda_b}^3}\Big(1-\frac{m_\tau^2}{q^2}\Big)^2,\\
A_1^{VA} &= |H^{VA}_{-1/2,1/2,+}|^2 + \sum|H^{VA}_{s,s,0}|^2 + |H^{VA}_{1/2,-1/2,-}|^2,\\
A_2^{VA} &= A_1^{VA} + 3\sum|H^{VA}_{s,s,t}|^2,\\
A_3^{SP} &= \sum|H^{SP}_{s,s}|^2,\\
A_4^{T} &= \sum|H^{T,s}_{s,t,0}|^2 + |H^{T,1/2}_{-1/2,t,-}|^2 + |H^{T,-1/2}_{1/2,t,+}|^2,\\
A_5^{VA-SP} &= \sum\Re[H^{SP*}_{s,s}H^{VA}_{s,s,t}],\\
A_6^{VA-T} &= \sum\Re[H^{VA*}_{s,s,0}H^{T,s}_{s,t,0}] + \Re[H^{VA*}_{-1/2,1/2,+}H^{T,-1/2}_{1/2,t,+}]\\
&\quad + \Re[H^{VA*}_{1/2,-1/2,-}H^{T,1/2}_{-1/2,t,-}],
\end{aligned} \tag{C15}$$

where $\sum$ depicts the summation over $s=\pm1/2$. For the forward-backward asymmetry in Eq. (16), we obtain

$$\frac{\mathrm{d}A_{\rm FB}}{\mathrm{d}q^2} = \frac{N_{\Lambda_c}}{\mathrm{d}\Gamma/\mathrm{d}q^2}\frac{3}{4}\Big[B_1^{VA} + \frac{2m_\tau^2}{q^2}(B_2^{VA}+8B_3^T) + \frac{2m_\tau}{\sqrt{q^2}}(B_4^{VA-SP}+4B_5^{VA-T}) + 8B_6^{SP-T}\Big], \tag{C16}$$

where

$$\begin{aligned}
B_1^{VA} &= |H^{VA}_{-1/2,1/2,+}|^2 - |H^{VA}_{1/2,-1/2,-}|^2,\\
B_2^{VA} &= \sum\Re[H^{VA*}_{s,s,t}H^{VA}_{s,s,0}],\\
B_3^{T} &= |H^{T,-1/2}_{1/2,t,+}|^2 - |H^{T,1/2}_{-1/2,t,-}|^2,\\
B_4^{VA-SP} &= \sum\Re[H^{SP*}_{s,s}H^{VA}_{s,s,0}],\\
B_5^{VA-T} &= \sum\Re[H^{VA*}_{s,s,t}H^{T,s}_{s,t,0}] + \Re[H^{VA*}_{-1/2,1/2,+}H^{T,-1/2}_{1/2,t,+}]\\
&\quad - \Re[H^{VA*}_{1/2,-1/2,-}H^{T,1/2}_{-1/2,t,-}],\\
B_6^{SP-T} &= \sum\Re[H^{SP*}_{s,s}H^{T,s}_{s,t,0}].
\end{aligned} \tag{C17}$$

For the Λ_c longitudinal polarization fraction in Eq. (17), we obtain

$$\frac{\mathrm{d}P_L^{\Lambda_c}}{\mathrm{d}q^2} = \frac{N_{\Lambda_c}}{\mathrm{d}\Gamma/\mathrm{d}q^2}\frac{1}{2}\Big[2C_1^{VA} + \frac{m_\tau^2}{q^2}C_2^{VA} + 3C_3^{SP} + 16\Big(1+\frac{2m_\tau^2}{q^2}\Big)C_4^T + 6\frac{m_\tau}{\sqrt{q^2}}(C_5^{VA-SP}+4C_6^{VA-T})\Big], \tag{C18}$$

where

$$\begin{aligned}
C_1^{VA} &= |H^{VA}_{1/2,1/2,0}|^2 - |H^{VA}_{-1/2,-1/2,0}|^2 + |H^{VA}_{-1/2,1/2,+}|^2 - |H^{VA}_{1/2,-1/2,-}|^2,\\
C_2^{VA} &= C_1^{VA} - 3|H^{VA}_{-1/2,-1/2,t}|^2 + 3|H^{VA}_{1/2,1/2,t}|^2,\\
C_3^{SP} &= |H^{SP}_{1/2,1/2}|^2 - |H^{SP}_{-1/2,-1/2}|^2,\\
C_4^{T} &= \sum 2s|H^{T,s}_{s,t,0}|^2 + |H^{T,-1/2}_{1/2,t,+}|^2 - |H^{T,1/2}_{-1/2,t,-}|^2,\\
C_5^{VA-SP} &= \sum 2s\Re[H^{SP*}_{s,s}H^{VA}_{s,s,t}],\\
C_6^{VA-T} &= \sum 2s\Re[H^{T,s}_{s,t,0}H^{VA*}_{s,s,0}] + \Re[H^{T,-1/2}_{1/2,t,+}H^{VA*}_{-1/2,1/2,+}]\\
&\quad - \Re[H^{T,1/2}_{-1/2,t,-}H^{VA*}_{1/2,-1/2,-}].
\end{aligned} \tag{C19}$$

For the τ-lepton longitudinal polarization fraction, we obtain

$$\frac{\mathrm{d}P_L^{\tau}}{\mathrm{d}q^2} = \frac{N_{\Lambda_c}}{\mathrm{d}\Gamma/\mathrm{d}q^2}\frac{1}{2}\Big[-2D_1^{VA} + \frac{m_\tau^2}{q^2}D_2^{VA} + 3D_3^{SP} + 16\Big(1-\frac{2m_\tau^2}{q^2}\Big)D_4^T + \frac{m_\tau}{\sqrt{q^2}}(6D_5^{VA-SP}-8D_6^{VA-T})\Big], \tag{C20}$$

where

$$\begin{aligned}
D_1^{VA} &= \sum|H^{VA}_{s,s,0}|^2 + |H^{VA}_{-1/2,1/2,+}|^2 + |H^{VA}_{1/2,-1/2,-}|^2,\\
D_2^{VA} &= D_1^{VA} + 3\sum|H^{VA}_{s,s,t}|^2,\\
D_3^{SP} &= \sum|H^{SP}_{s,s}|^2,\\
D_4^{T} &= \sum|H^{T,s}_{s,t,0}|^2 + |H^{T,-1/2}_{1/2,t,+}|^2 + |H^{T,1/2}_{-1/2,t,-}|^2,\\
D_5^{VA-SP} &= \sum\Re[H^{SP*}_{s,s}H^{VA}_{s,s,t}],\\
D_6^{VA-T} &= \sum\Re[H^{T,s}_{s,t,0}H^{VA*}_{s,s,0}] + \Re[H^{T,-1/2}_{1/2,t,+}H^{VA*}_{-1/2,1/2,+}]\\
&\quad + \Re[H^{T,1/2}_{-1/2,t,-}H^{VA*}_{1/2,-1/2,-}].
\end{aligned} \tag{C21}$$

References

1 Y. Li and C.-D. L, Sci. Bull., **63**: 267-269 (2018), arXiv:1808.02990
2 S. Bifani, S. Descotes-Genon, A. Romero Vidal et al, J. Phys. G, **46**(2): 023001 (2019), arXiv:1809.06229
3 BaBar Collaboration, J. P. Lees et al, Phys. Rev. Lett., **109**: 101802 (2012), arXiv:1205.5442
4 BaBar Collaboration, J. P. Lees et al, Phys. Rev. D, **88**(7): 072012 (2013), arXiv:1303.0571
5 Belle Collaboration, M. Huschle et al, Phys. Rev. D, **92**(7): 072014 (2015), arXiv:1507.03233
6 Belle Collaboration, Y. Sato et al, Phys. Rev. D, **94**(7): 072007 (2016), arXiv:1607.07923
7 Belle Collaboration, S. Hirose et al, Phys. Rev. Lett., **118**(21): 211801 (2017), arXiv:1612.00529
8 Belle Collaboration, S. Hirose et al, Phys. Rev. D, **97**(10): 12004 (2018), arXiv:1709.00129
9 LHCb Collaboration, R. Aaij et al, Phys. Rev. Lett., **115**(11): 111803 (2015), arXiv:1506.08614
10 LHCb Collaboration, R. Aaij et al, Phys. Rev. Lett., **120**(17): 171802 (2018), arXiv:1708.08856
11 LHCb Collaboration, R. Aaij et al, Phys. Rev. D, **97**(7): 072013 (2018), arXiv:1711.02505
12 Heavy Flavor Averaging Group Collaboration, Y. Amhis et al, Eur. Phys. J. C, **77**: 895 (2017), arXiv:1612.07233
13 D. Bigi and P. Gambino, Phys. Rev. D, **94**(9): 094008 (2016), arXiv:1606.08030
14 S. Jaiswal, S. Nandi, and S. K. Patra, JHEP, **12**: 060 (2017), arXiv:1707.09977
15 F. U. Bernlochner, Z. Ligeti, M. Papucci et al, Phys. Rev. D, **95**(11): 115008 (2017), arXiv:1703.05330
16 D. Bigi, P. Gambino, and S. Schacht, JHEP, **11**: 061 (2017), arXiv:1707.09509
17 LHCb Collaboration, R. Aaij et al, Phys. Rev. Lett., **120**(12): 121801 (2018), arXiv:1711.05623
18 W. Wang, Y.-L. Shen, and C.-D. Lu, Phys. Rev. D, **79**: 054012 (2009), arXiv:0811.3748
19 LHCb Collaboration, R. Aaij et al, Phys. Rev. Lett., **113**: 151601 (2014), arXiv:1406.6482
20 LHCb Collaboration, R. Aaij et al, JHEP, **08**: 055 (2017), arXiv:1705.05802
21 G. Hiller and F. Kruger, Phys. Rev. D, **69**: 074020 (2004), arXiv:hep-ph/0310219

22 M. Bordone, G. Isidori, and A. Pattori, Eur. Phys. J. C, **76**(8): 440 (2016), arXiv:1605.07633
23 Y. Sakaki, M. Tanaka, A. Tayduganov et al, Phys. Rev. D, **91**(11): 114028 (2015), arXiv:1412.3761
24 B. Bhattacharya, A. Datta, D. London et al, Phys. Lett. B, **742**: 370-374 (2015), arXiv:1412.7164
25 L. Calibbi, A. Crivellin, and T. Ota, Phys. Rev. Lett., **115**: 181801 (2015), arXiv:1506.02661
26 F. Feruglio, P. Paradisi, and A. Pattori, Phys. Rev. Lett., **118**(1): 011801 (2017), arXiv:1606.00524
27 D. Choudhury, A. Kundu, R. Mandal et al, Phys. Rev. Lett., **119**(15): 151801 (2017), arXiv:1706.08437
28 Q.-Y. Hu, X.-Q. Li, and Y.-D. Yang, *$b \to c\tau\nu$ Transitions in the Standard Model Effective Field Theory*, arXiv: 1810.04939
29 A. Celis, M. Jung, X.-Q. Li et al, JHEP, **01**: 054 (2013), arXiv:1210.8443
30 N. G. Deshpande and X.-G. He, Eur. Phys. J. C, **77**(2): 134 (2017), arXiv:1608.04817
31 A. Celis, M. Jung, X.-Q. Li et al, Phys. Lett. B, **771**: 168-179 (2017), arXiv:1612.07757
32 J. Zhu, B. Wei, J.-H. Sheng et al, Nucl. Phys. B, **934**: 380-395 (2018), arXiv:1801.00917
33 S.-P. Li, X.-Q. Li, Y.-D. Yang et al, JHEP, **09**: 149 (2018), arXiv:1807.08530
34 Q.-Y. Hu, X.-Q. Li, Y. Muramatsu et al, Phys. Rev. D, **99**(1): 015008 (2019), arXiv:1808.01419
35 W. Altmannshofer, P. S. Bhupal Dev, and A. Soni, Phys. Rev. D, **96**(9): 095010 (2017), arXiv:1704.06659
36 A. K. Alok, D. Kumar, S. Kumbhakar et al, arXiv: 1903.10486
37 T. Mandal, S. Mitra, and S. Raz, Phys. Rev. D, **99**(5): 055028 (2019), arXiv:1811.03561
38 C.-T. Tran, M. A. Ivanov, J. G. Körner et al, Phys. Rev. D, **97**(5): 054014 (2018), arXiv:1801.06927
39 D. Bečirević, S. Fajfer, N. Košnik et al, Phys. Rev. D, **94**(11): 115021 (2016), arXiv:1608.08501
40 D. Das, C. Hati, G. Kumar et al, Phys. Rev. D, **96**(9): 095033 (2017), arXiv:1705.09188
41 M. Blanke and A. Crivellin, Phys. Rev. Lett., **121**(1): 011801 (2018), arXiv:1801.07256
42 N. Assad, B. Fornal, and B. Grinstein, Phys. Lett. B, **777**: 324-331 (2018), arXiv:1708.06350
43 K. Azizi, Y. Sarac, and H. Sundu, arXiv: 1904.08267
44 R. Dutta, A. Bhol, and A. K. Giri, Phys. Rev. D, **88**(11): 114023 (2013), arXiv:1307.6653
45 B. Fornal, S. A. Gadam, and B. Grinstein, Phys. Rev. D, **99**(5): 055025 (2019), arXiv:1812.01603
46 Belle, Belle II Collaboration, K. Adamczyk, *Semitauonic B decays at Belle/Belle II, in 10th International Workshop on the CKM Unitarity Triangle (CKM 2018) Heidelberg, Germany, September 17-21, 2018*, 2019. arXiv: 1901.06380
47 Belle Collaboration, A. Abdesselam et al, *Measurement of the D^{*-} polarization in the decay $B^0 \to D^{*-}\tau^+\nu\tau$*, arXiv: 1903.03102
48 A. K. Alok, D. Kumar, S. Kumbhakar et al, Phys. Rev. D, **95**(11): 115038 (2017), arXiv:1606.03164
49 Z.-R. Huang, Y. Li, C.-D. Lu et al, Phys. Rev. D, **98**(9): 095018 (2018), arXiv:1808.03565
50 J. Aebischer, J. Kumar, P. Stangl et al, *A Global Likelihood for Precision Constraints and Flavour Anomalies*, arXiv: 1810.07698
51 M. Blanke, A. Crivellin, S. de Boer et al, *Impact of polarization observables and $B_c \to \tau\nu$ on new physics explanations of the $b \to c\tau\nu$ anomaly*, arXiv: 1811.09603
52 S. Iguro, T. Kitahara, Y. Omura et al, JHEP, **02**: 194 (2019), arXiv:1811.08899
53 M. Tanaka and R. Watanabe, Phys. Rev. D, **87**(3): 034028 (2013), arXiv:1212.1878
54 Belle II Collaboration, W. Altmannshofer et al, *The Belle II Physics Book*, arXiv: 1808.10567
55 LHCb Collaboration, R. Aaij et al., *Physics case for an LHCb Upgrade II - Opportunities in flavour physics, and beyond, in the HL-LHC era*, arXiv: 1808.08865
56 A. Crivellin, D. Mller, and T. Ota, JHEP, **09**: 040 (2017), arXiv:1703.09226
57 I. Dorner, S. Fajfer, A. Greljo et al, Phys. Rept., **641**: 1-68 (2016), arXiv:1603.04993
58 M. Freytsis, Z. Ligeti, and J. T. Ruderman, Phys. Rev. D, **92**(5): 054018 (2015), arXiv:1506.08896
59 M. Bauer and M. Neubert, Phys. Rev. Lett., **116**(14): 141802 (2016), arXiv:1511.01900
60 X.-Q. Li, Y.-D. Yang, and X. Zhang, JHEP, **02**: 068 (2017), arXiv:1611.01635
61 S. Fajfer and N. Konik, Phys. Lett. B, **755**: 270-274 (2016), arXiv:1511.06024
62 F. F. Deppisch, S. Kulkarni, H. Ps et al, Phys. Rev. D, **94**(1): 013003 (2016), arXiv:1603.07672
63 B. Dumont, K. Nishiwaki, and R. Watanabe, Phys. Rev. D, **94**(3): 034001 (2016), arXiv:1603.05248
64 L. Di Luzio, A. Greljo, and M. Nardecchia, Phys. Rev. D, **96**(11): 115011 (2017), arXiv:1708.08450
65 Y. Cai, J. Gargalionis, M. A. Schmidt et al, JHEP, **10**: 047 (2017), arXiv:1704.05849
66 L. Calibbi, A. Crivellin, and T. Li, Phys. Rev. D, **98**(11): 115002 (2018), arXiv:1709.00692
67 J. Kumar, D. London, and R. Watanabe, Phys. Rev. D, **99**(1): 015007 (2019), arXiv:1806.07403
68 C. Hati, G. Kumar, J. Orloff et al, JHEP, **11**: 011 (2018), arXiv:1806.10146
69 A. Crivellin, C. Greub, D. Mller et al, Phys. Rev. Lett., **122**(1): 011805 (2019), arXiv:1807.02068
70 A. Angelescu, D. Beirevi, D. A. Faroughy et al, JHEP, **10**: 183 (2018), arXiv:1808.08179
71 T. J. Kim, P. Ko, J. Li et al, *Correlation between $R_{D(*)}$ and top quark FCNC decays in leptoquark models*, arXiv: 1812.08484
72 D. Marzocca, JHEP, **07**: 121 (2018), arXiv:1803.10972
73 D. Buttazzo, A. Greljo, G. Isidori et al, JHEP, **11**: 044 (2017), arXiv:1706.07808
74 P. Arnan, D. Becirevic, F. Mescia et al, JHEP, **02**: 109 (2019), arXiv:1901.06315
75 W. Detmold, C. Lehner, and S. Meinel, Phys. Rev. D, **92**(3): 034503 (2015), arXiv:1503.01421
76 A. Datta, S. Kamali, S. Meinel et al, JHEP, **08**: 131 (2017), arXiv:1702.02243
77 Flavour Lattice Averaging Group Collaboration, S. Aoki et al, *FLAG Review 2019*, arXiv: 1902.08191
78 A. Cerri et al, *Opportunities in Flavour Physics at the HL-LHC and HE-LHC*, arXiv: 1812.07638
79 K. Hagiwara, A. D. Martin, and M. F. Wade, Nucl. Phys. B, **327**: 569-594 (1989)
80 F. U. Bernlochner, Z. Ligeti, and D. J. Robinson, *N = 5, 6, 7, 8: Nested hypothesis tests and truncation dependence of |Vcb|*, arXiv: 1902.09553
81 Y.-M. Wang, Y.-B. Wei, Y.-L. Shen et al, JHEP, **06**: 062 (2017), arXiv:1701.06810
82 N. Gubernari, A. Kokulu, and D. van Dyk, JHEP, **01**: 150 (2019), arXiv:1811.00983
83 C. W. Murphy and A. Soni, Phys. Rev. D, **98**(9): 094026 (2018), arXiv:1808.05932
84 A. Berns and H. Lamm, JHEP, **12**: 114 (2018), arXiv:1808.07360
85 W. Wang and R. Zhu, *Model independent investigation of the $R_{J/\psi,\,\eta c}$ and ratios of decay widths of semileptonic Bc decays into a P-wave charmonium*, arXiv: 1808.10830
86 D. Leljak, B. Melic, and M. Patra, *On lepton flavour universality in semileptonic $Bc \to \eta_c, J/\psi$ decays*, arXiv: 1901.08368
87 T. Gutsche, M. A. Ivanov, J. G. Krner et al, Phys. Rev. D, **91**(7): 074001 (2015), arXiv:1502.04864
88 C. G. Boyd, B. Grinstein, and R. F. Lebed, Phys. Rev. D, **56**: 6895-6911 (1997), arXiv:hep-ph/9705252

89 I. Caprini, L. Lellouch, and M. Neubert, Nucl. Phys. B, **530**: 153-181 (1998), arXiv:hep-ph/9712417
90 G. Buchalla, A. J. Buras, and M. E. Lautenbacher, Rev. Mod. Phys., **68**: 1125-1144 (1996), arXiv:hep-ph/9512380
91 W. Altmannshofer and D. M. Straub, *Implications of $b \to s$ measurements, in Proceedings, 50th Rencontres de Moriond Electroweak Interactions and Unified Theories: La Thuile, Italy, March 14-21, 2015*, pp. 333–338, 2015. arXiv: 1503.06199
92 S. Descotes-Genon, L. Hofer, J. Matias et al, JHEP, **06**: 092 (2016), arXiv:1510.04239
93 T. Hurth, F. Mahmoudi, and S. Neshatpour, Nucl. Phys. B, **909**: 737-777 (2016), arXiv:1603.00865
94 Muon g-2 Collaboration, G. W. Bennett et al, Phys. Rev. D, **73**: 072003 (2006), arXiv:hep-ex/0602035
95 Particle Data Group Collaboration, M. Tanabashi et al, Phys. Rev. D, **98**(3): 030001 (2018)
96 CMS Collaboration, A. M. Sirunyan et al, Phys. Rev. Lett., **121**(24): 241802 (2018), arXiv:1809.05558
97 ATLAS Collaboration, M. Aaboud et al, *Searches for third-generation scalar leptoquarks in $\sqrt{s}$ = 13 TeV pp collisions with the ATLAS detector*, arXiv: 1902.08103
98 CKMfitter Group Collaboration, J. Charles, A. Hocker, H. Lacker, S. Laplace, F. R. Le Diberder, J. Malcles, J. Ocariz, M. Pivk, and L. Roos, Eur. Phys. J. C, **41**(1): 1-131 (2005)
99 M. Jung, X.-Q. Li, and A. Pich, JHEP, **10**: 063 (2012), arXiv:1208.1251
100 C.-W. Chiang, X.-G. He, F. Ye et al, Phys. Rev. D, **96**(3): 035032 (2017), arXiv:1703.06289
101 LHCb Collaboration, R. Aaij et al, Phys. Rev. Lett., **118**(25): 251802 (2017), arXiv:1703.02508
102 C. Bobeth, M. Gorbahn, T. Hermann et al, Phys. Rev. Lett., **112**: 101801 (2014), arXiv:1311.0903
103 J. Albrecht, F. Bernlochner, M. Kenzie et al, *Future prospects for exploring present day anomalies in flavour physics measurements with Belle II and LHCb*, arXiv: 1709.10308
104 J. F. Kamenik, S. Monteil, A. Semkiv et al, Eur. Phys. J. C, **77**(10): 701 (2017), arXiv:1705.11106
105 Belle Collaboration, G. *Caria, Measurement of $R(D)$ and $R(D^*)$ with a semileptonic tag at Belle*, Talk at '54th Rencontres de Moriond, Electroweak Interactions and Unified Theories, 2019'
106 elle Collaboration, A. Abdesselam et al., *Measurement of $\mathcal{R}(D)$ and $\mathcal{R}(D^*)$ with a semileptonic tagging method*, arXiv: 1904.08794
107 C. Murgui, A. Peuelas, M. Jung et al, *Global fit to $b \to c\tau\nu$ transitions*, arXiv: 1904.09311
108 J. G. Korner and G. A. Schuler, Z. Phys. C, **46**: 93 (1990)
109 H. E. Haber, *Spin formalism and applications to new physics searches, in Spin structure in high-energy processes: Proceedings, 21st SLAC Summer Institute on Particle Physics, 26 Jul - 6 Aug 1993, Stanford*, CA, pp. 231–272, 1994. hep-ph/9405376
110 Y. Sakaki, M. Tanaka, A. Tayduganov et al, Phys. Rev. D, **88**(9): 094012 (2013), arXiv:1309.0301
111 D. Bardhan, P. Byakti, and D. Ghosh, JHEP, **01**: 125 (2017), arXiv:1610.03038